Optimizing Spatial On-street Parking Provision for Logistic Vehicles

Amirreza Pashapour [*], Barış Yıldız [†]

Abstract

Curbside management must simultaneously accommodate both logistic and passenger vehicles claiming access to limited on-street parking spaces. We study the novel Spatial On-street Parking Provision (SOPP) problem that jointly optimizes the parking reservation count and its spatial placement along the curbside. SOPP enables efficient, location-aware parking space reservation for logistic vehicles in a bi-modal system comprising logistic and passenger vehicles to promote sustainable urban traffic. Here, logistic vehicles park in any reserved or unreserved space within a walking-distance threshold of their target commercial establishment, while passenger vehicles use the remaining unreserved parking capacity. We formulate SOPP as a bilevel model. The upper level determines the parking reservation policy, while the lower level embeds a continuous-time Markov chain (CTMC) to capture curbside occupancy dynamics and evaluate the resulting probabilities of parking configurations. This structure allows us to quantify the externalities from blocked parking and the system-wide costs. Given the complexity of the exact model, we develop a tractable machine-learning surrogate based on a quadratic Boolean approximation, trained on CTMC outputs and subsequently replacing the embedded CTMC in the optimization. The framework can be extended to relax the assumptions on arrival and parking-duration distributions, and it accommodates both same-side and flexible cross-street parking policies. Our comprehensive numerical experiments with real-world data show the efficacy of the suggested approach and provide critical insights. Our proposed SOPP approach outperforms the location-ignorant benchmark, achieving 15% improvement under a baseline test case and 30% improvement in a traffic-intensive scenario. Sensitivity analysis indicates that the arrival rate ratio of logistic to passenger vehicles is the primary driver of reservation decisions, while the walking distance threshold, blocking cost coefficients, and departure rate ratios exert secondary effects.

Keywords: Urban parking, Logistic vehicles, Street parking, Parking provision, Surrogate modeling, Machine learning

1 Introduction

Curbside space has long been a limited resource in cities. Rapid growth in private vehicle ownership, coupled with the accelerating expansion of urban logistics driven by e-commerce expansion, shorter delivery lead times, and more frequent small shipments, is intensifying demand for curb access (Chiara et al. 2020,

[*]School of Management, University of Bath, Bath BA2 7AY, United Kingdom; Email: ap3903@bath.ac.uk
[†]Department of Industrial Engineering, Koç University, Istanbul 34450, Türkiye; Email: byildiz@ku.edu.tr

Castrellon & Sanchez-Diaz 2024, Liu & Qian 2024). For example, Eurostat (2026) report a 6.3% increase in registered passenger cars in the EU between 2019 and 2024. Meanwhile, World Economic Forum (2020) project a 36% increase in delivery vehicle volumes by 2030 across the world's 100 largest cities.

In response to these competing pressures, cities are increasingly considering the provision of dedicated parking bays for logistic vehicles. Data shows that such targeted allocations can yield operational and environmental benefits. From their field experiment in Querétaro, Mexico, Fransoo et al. (2022) find that maintaining unloading bays exclusively for freight operations results in 39% and 17% reductions in travel time and total parking time, respectively. Similarly, Mora-Quiñones et al. (2024) report reductions of up to 3.55 percent in morning CO_2 levels and a 14 percent decrease in noise following the establishment of dedicated loading and unloading bays according to their field experiment in Zapopan, Mexico.

A natural policy response is to increase the number of on-street spaces reserved for logistic vehicles. However, two critical considerations arise. First, the curbside supply is fixed. Reserving additional space for freight inevitably reduces capacity available for general parking and other curbside uses. Such allocations frequently generate resistance from passenger vehicle users and public transport operators (Nourinejad et al. 2014, Abhishek et al. 2021). Even the traffic effects of expanding the logistics bay area are not unambiguously positive. Liu et al. (2024) find that adding 100 curbside logistics parking units in a region decreases overall traffic speed by 3.70 mph on weekdays and 4.54 mph on weekends on average. The alternative is equally problematic. When no legal options exist, many logistic vehicle drivers double park or park illegally on, for example, travel lanes, no stopping zones, cycle lanes, or bus stops (Ghizzawi et al. 2024). Such practices are prevalent because logistic vehicle drivers avoid cruising due to the associated costs and delivery delays (e Silva & Alho 2017). This generates spillover effects throughout the urban transport network and imposes negative externalities. Han et al. (2005) show that logistic vehicles stopping in travel lanes rank as the third leading cause of non-recurrent urban congestion, behind only crashes and construction, with an estimated $10 billion in annual delay costs in the United States. Second, beyond sizing the logistics parking bay capacity, determining the specific locations of the reserved spaces along the curbside is equally critical. This directly affects walking distances to commercial establishments, handling times, and overall delivery productivity. Even when the total reservation capacity is well calibrated, inefficient spatial allocation may erode operational benefits.

Notably, although passenger and logistic vehicles compete for the same scarce curb space, their parking needs and the externalities they generate differ fundamentally. Passenger vehicles require longer-duration parking and, when spaces are unavailable, drivers often cruise in search of an open spot. Empirical evidence suggests that cruising for parking can account for up to 15% of urban traffic in dense districts (Hampshire & Shoup 2018). logistic vehicles, in contrast, rely on short but frequent stops at specific destinations to conduct loading and unloading operations. Their parking locations are considerably less flexible, as deliveries must occur in close proximity to customer premises and within strict time windows. Field studies conducted in Querétaro, Mexico (Fransoo et al. 2022) and Seattle, Washington (Dalla Chiara et al. 2021) report that logistic vehicles spend approximately 80% of their operating time parked in dense urban environments. It is not uncommon for a delivery route to involve over 60 stops (Fransoo et al. 2022). Accounting for these structural differences is critical to designing effective curbside parking management that support sustainable

urban commerce and service operations (Vieira & Fransoo 2015, Kin et al. 2017).

To address these challenges, we study the SOPP under bimodal parking demand from passenger and logistic vehicles. We consider a street segment with on-street parking spaces and commercial establishments, such as retail stores, food and beverage, health or accommodation services, etc., that generate freight demand. Arrivals and parking durations for both vehicle types are stochastic. In this context, SOPP aims to reserve a subset of curbside parking spaces exclusively for logistic vehicles, fostering a win-win environment for both logistic and passenger vehicles. Our objective is to minimize system costs resulting from parking blockages, which induce illegal parking among logistic vehicles and cruising among passenger vehicles.

Our study contributes to the literature on on-street parking problems (OPP) from three main perspectives. Operationally, SOPP extends the aggregate parking provision frameworks of Abhishek et al. (2021), Legros & Fransoo (2024), and Darendeliler et al. (2026) along two important dimensions. First, motivated by the last-mile delivery constraint (Goodchild & Ivanov 2017, Amer & Chow 2017), logistic vehicles park within a walking distance threshold, $\overline{d}$, of their destination. Accordingly, each establishment $j \in \mathcal{J}$ can be served only by a localized subset of (reserved or unreserved) parking spaces, denoted by δ_j, while passenger vehicles can uniformly use any unreserved space. This spatial constraint gives rise to a more complex multi-rate parking server pool (effective arrival rates to parking spaces depend endogenously on spatial reservation decisions) embedded in an Erlang loss system (there is no waiting for an occupied parking space). Second, the existing literature assumes a sequential overflow structure: logistic vehicles first attempt to park in a designated bay and, only if it is full, spill over to general-use parking spaces. This imposes a strict priority ordering. We relax this assumption by allowing logistic vehicle drivers to choose freely among available spaces (reserved or unreserved), based on proximity or convenience. In practice, a driver may prefer an empty general-use space over an empty reserved parking space if the former is closer to their destination. That said, the parking space reservation acts as a demand regulation mechanism rather than enforcing a rigid sequential assignment rule. Under these two modeling principles, existing aggregate OPP models emerge as special cases of SOPP when $\overline{d} \to \infty$ and sequential assignment is restored.

From a methodological standpoint, we formulate SOPP as a bilevel optimization problem in which the upper level determines the parking space reservations, while the lower level embeds a CTMC to evaluate location-dependent blocking probabilities and the resulting total system cost. To address the computational complexity, we develop a novel approximation approach that replaces the computationally prohibitive lower-level Markovian evaluation with a tractable surrogate based on a quadratic Boolean approximation. As we show in our numerical experiments, this approach can solve otherwise intractable problem instances quite efficiently. The proposed methodology naturally extends to a broader class of transportation planning problems, such as the placement of on-street EV charging stations and ambulance stationing, where similar bilevel structures arise.

From the experimentation aspect, we conduct extensive numerical studies with real-world data to test the efficacy of the suggested approach, derive managerial insights, and ultimately answer the two central questions: ii) *How does SOPP perform compared to location-ignorant aggregate parking allocation approaches in terms of total system performance?* and ii) *How sensitive are optimal SOPP decisions with respect to key demand and operational parameters?* We find that due to strong spatial overlap among

parking spaces, reserving one space reshapes passenger and logistic vehicles' parking demand distribution and blocking probabilities elsewhere, rendering simple threshold or sequential additive rules suboptimal. Loose reservations not only remain underutilized and fail to support last-mile operations effectively, but also, we demonstrate that they can, counterintuitively, increase illegal parking by logistic vehicles along the street. Moreover, our results show that the location-ignorant approach can perform poorly: in our test case, it suggests zero reservations and results in a 15% performance gap relative to our method, exceeding 30% under further traffic-intensive conditions. Our sensitivity analysis reveals that both reservation levels and total cost vary approximately linearly with the passenger-to-logistic arrival ratio, while showing diminishing marginal effects with respect to the walking distance threshold, cost coefficient ratio, and departure rate ratio.

Figure 1 illustrates a representative street with heterogeneous freight demand across establishments (indicated by varying color intensities). For instance, parking spaces 1, 2, and 3 are operationally feasible for serving establishment 1, whereas more distant spaces are infeasible under the threshold $\overline{d}$. In the depicted configuration, spaces 3 and 7 are reserved exclusively for logistic vehicles (highlighted in green), restricting passenger access. From the perspective of a municipal or public agency decision-maker, the objective is to determine a reservation scheme that minimizes the total blocking costs incurred by both logistic and passenger vehicles, while avoiding excessive reservations that would unduly restrict passenger parking supply. As we find later, simple threshold-based or sequential additive rules remain suboptimal in the SOPP setting.

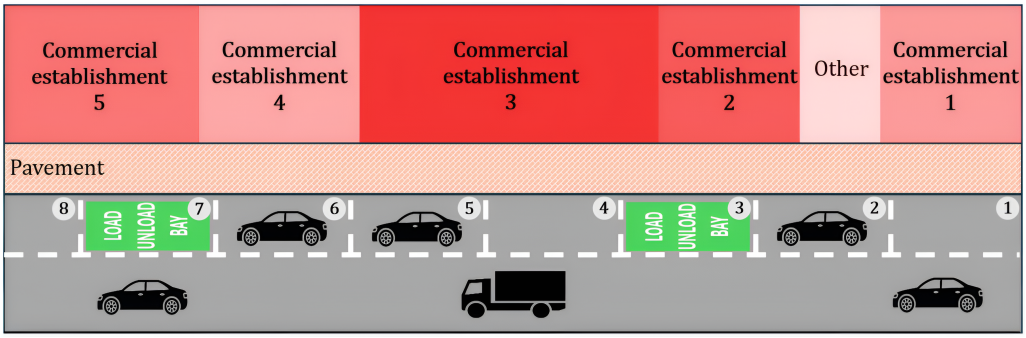

Figure 1: Schematic representation of the SOPP. Commercial establishments generate heterogeneous freight demand (color intensity), and logistic vehicles must park within a feasible localized parking space set based on the walking distance threshold $\overline{d}$. Selected spaces (green) are reserved exclusively for logistic vehicles, while remaining spaces are shared with passenger vehicles.

The rest of the paper is organized as follows. We position the SOPP within the OPP literature and provide an overview of relevant studies in Section 2. Section 3 formulates a compact bi-level optimization model that embeds a CTMC submodel and analyzes its structural properties. We propose our machine learning-based surrogate modeling methodology in Section 4. Section 5 establishes a real-world test case, presents numerical results, evaluates our model across varying total parking spaces reserved, and conducts cross-validation using an example from the literature. Section 6 conducts a comprehensive sensitivity analysis to derive managerial insights for SOPP policies under varying street dynamics and summarizes our key findings. Finally, Section 7 presents concluding remarks.

2 Literature Review

We position our study within three research streams on OPP. The first stream focuses on understanding parking demand and the behavior of passenger and logistic vehicles through empirical or simulation analyses. These studies document substantial curbside pressures and frequent illegal parking by logistic vehicles (Schmid et al. 2018, Chiara et al. 2020, Kim & Wang 2022), propose methods to estimate search times for on-street parking (Fulman & Benenson 2021, Dutta et al. 2023), model curbside usage by considering users' route choices, curb space competition, and their interactive effects (Liu & Qian 2024) and highlight the role of demand management and dedicated loading space in improving freight operations (Campbell et al. 2018, Silva et al. 2020, Fransoo et al. 2022, Darendeliler et al. 2026). Building on the findings and insights from this stream, we develop an optimization framework to determine reservation decisions for logistic vehicles' parking spaces in a shared competitive curbside environment.

A second group of OPP-related studies integrates parking decisions into last-mile delivery operations. These studies typically embed decisions about parking choice or provision within vehicle routing or operational optimization models. For example, Liu et al. (2023) study the Freight Parking Management Problem, where delivery drivers jointly determine routes and parking choices in real time, while Reed et al. (2024) incorporate parking times explicitly into a vehicle routing formulation that minimizes total delivery completion time. Similarly, Ismael & Holguin-Veras (2025) develop a real-time allocation model that assigns heterogeneous vehicles to available parking spaces to minimize travel times, and Burns et al. (2025) investigate dynamic parking reservation systems to better accommodate delivery demand. While these studies provide important insights into the operational management of the logistics bay area and its interaction with delivery routing, our focus is different. Rather than modeling logistics operations, we study the planning problem from the perspective of a public agency that determines which curbside spaces to reserve for logistic vehicles in order to reduce the negative externalities arising from insufficient parking for both logistic and passenger vehicles.

The third, and most extensively studied, stream of OPP research is rooted in queueing theory. These models are generally street-specific, and the *M/M/c/c* structure is the most commonly examined framework (Caliskan et al. 2007, Dalla Chiara & Cheah 2017, Dowling et al. 2019, Abdeen et al. 2021, Abhishek et al. 2021, Legros & Fransoo 2024). Xiao et al. (2018) demonstrate that loss queue models effectively estimate system parameters and predict parking occupancy. Abhishek et al. (2021) evaluate the performance of a mixed-use parking system serving delivery and passenger vehicles using a loss queue framework. More recently, Legros & Fransoo (2024) model a parking lot where delivery vehicles arrive exogenously and park for free, while passenger vehicle arrivals depend on price and availability. The frameworks of Abhishek et al. (2021) and Legros & Fransoo (2024) partition the total on-street parking capacity c into c_b and c_s spaces for logistic and passenger vehicles, respectively, such that $c_b + c_s = c$ (with the latter study incorporating pricing decisions). In their setting, a logistic vehicle first attempts to park in a logistics bay; if all are occupied, it overflows into the passenger bay. Passenger vehicles, by contrast, can only use passenger bays. This leads to two Erlang loss systems: an $M/M/c_b/c_b$ queue for logistic vehicles and a $GI + M/M/c_s/c_s$ queue for passenger vehicles, where GI represents the renewal process of overflow logistics arrivals. Using a similar

partitioning, Darendeliler et al. (2026) study a dynamic parking space allocation problem (DyPARK). The authors develop a data-driven Markov decision process model to construct an optimal admission control policy that decides whether to accept or reject an arriving vehicle based on the current system dynamics. Apart from the above stream, our study incorporates demand from commercial establishments and optimizes the spatial distribution of reserved curbside parking spaces for logistic vehicles. Moreover, we model the arrivals of logistic and passenger vehicles flexibly, where logistic vehicle drivers arbitrarily choose an available parking space rather than imposing a rigid sequential overflow rule from reserved bays to shared spaces. Following the similar queuing structure in the literature, we employ a bi-level formulation in which an *M/M/c/c*-based CTMC model is embedded to capture system dynamics. We also propose a scalable, precise, and fast machine-learning-based surrogate model that is generalizable and can accommodate non-Markovian arrivals.

3 Mathematical Model

In Section 3.1, we formally define the OPP problem for urban logistic vehicles. Section 3.2 develops a CTMC submodel that is subsequently embedded within our bilevel optimization model. Section 3.3 derives the objective function, which minimizes the negative societal externalities associated with the costs of logistic vehicles' illegal parking events and passenger vehicles' cruising events, both due to a blocked parking effort. Finally, Section 3.4 presents the ensuing bi-level optimization model, together with a discussion of its size and structural properties. Table 1 provides a glossary of notations as a quick reference.

Table 1: Glossary of notations

Notation	Description
Sets:	
$\mathcal{I}$	Set of curb-side parking spaces along a street
$\mathcal{J}$	Set of commercial establishments along a street
$\mathcal{S}(\mathbf{x})$	State space set of all possible parking configurations of parked vehicles along a street as a function of $\mathbf{x}$ state space
$\mathcal{F}_{1j}(s)$	Set of free spaces available to a logistic vehicle when targeting establishment $j \in \mathcal{J}$ under state $s \in \mathcal{S}(\mathbf{x})$
$\mathcal{F}_2^{\mathbf{x}}(s)$	Set of free spaces available to passenger vehicles under state s and reservation $\mathbf{x}$
δ_j	Set of parking spaces located within a walking distance threshold $\overline{d}$ from the establishment $j \in \mathcal{J}$
$\mathcal{K}$	Set of tuples of parking spaces that serve at least one common establishment, i.e., $\mathcal{K} = \{(i,i') \in \mathcal{I} \times \mathcal{I} : i < i' \wedge \exists\, j \in \mathcal{J} : i, i' \in \delta_j\}$
Parameters:	
d_{ij}	Walking distance of parking space $i \in \mathcal{I}$ from establishment $j \in \mathcal{J}$
$\overline{d}$	Walking distance threshold
λ_1	Steady-state arrival rate of logistic vehicles
λ_{1j}	Steady-state arrival rate of logistic vehicles for delivery to establishment $j \in \mathcal{J}$
λ_2	Steady-state arrival rate of passenger vehicles with parking demand
μ_1	Parking duration rate of logistic vehicles (vehicles per time unit)
μ_2	Parking duration rate of passenger vehicles (vehicles per time unit)
α_1	Unit cost of blocked parking of a logistic vehicle
α_2	Unit cost of blocked parking of a passenger vehicle
$Q(\mathbf{x})$	Reservation-dependent CTMC generator matrix
Decision variables:	
x_i	1, if parking space $i \in \mathcal{I}$ is updated to premium; 0, otherwise
$\pi_s(\mathbf{x})$	Steady-state reservation-dependent probabilities associated with state $s \in \mathcal{S}(\mathbf{x})$

3.1 Problem Overview

Consider a street with curbside parking spaces indexed by $i \in \mathcal{I}$. Along this street lies a set of distinct commercial establishments $j \in \mathcal{J}$ that generate logistic vehicle demand. A centralized decision maker (e.g., a public parking authority) seeks to determine a subset of parking spaces $i \in \mathcal{I}$ to allocate exclusively to logistic vehicles, prohibiting passenger vehicles from parking there. We define a binary reservation vector $\mathbf{x} \in \{0,1\}^{|\mathcal{I}|}$, where $x_i = 1$ if parking space $i \in \mathcal{I}$ is reserved for logistic vehicles only, and $x_i = 0$ if it remains available for general use of either entities.

The following set of principles is adopted to establish a stylized model, unless noted otherwise:

- *Interaction of parking locations with commercial establishments*: We define the set δ_j, which includes parking spaces that serve as a feasible parking option for delivery to establishment $j \in \mathcal{J}$, considering he walking distance threshold. Formally,

$$\delta_j = \{i \in \mathcal{I} : d_{ij} \leq \overline{d}\} \quad \forall j \in \mathcal{J}. \tag{1}$$

  Here, d_{ij} represents the Euclidean walking distance from parking space $i \in \mathcal{I}$ to establishment $j \in \mathcal{J}$, and $\overline{d}$ is an arbitrary last-mile delivery walking threshold for logistic vehicle drivers.

- *Street dynamics*: For ease of exposition, let λ_{1j} denote the arrival rate of logistic vehicles for delivery to establishment $j \in \mathcal{J}$, and λ_2 denote the arrival rate of passenger vehicles, both assumed to be asymptotic and follow Poisson processes. Also, let $\lambda_1 = \sum_{j \in \mathcal{J}} \lambda_{1j}$ denote the total arrival rate of logistic vehicles to the street. Parking durations for logistic and passenger vehicles are exponentially distributed with service rates μ_1 and μ_2 (vehicles per unit time), respectively. Later, we will conduct a sensitivity analysis on the effect of varying arrival and departure rates on reservation decisions in Section 6. Markovian assumptions on these parameters can be relaxed when implementing our surrogate modeling framework, as described in Section 4.

- *Parking distribution*: logistic vehicles targeting establishment $j \in \mathcal{J}$ park uniformly among δ_j parking spaces. Similarly, passenger vehicles uniformly park at any available, unreserved parking space.

The above-mentioned features yield a novel, more granular SOPP formulation for logistic vehicles, at the expense of increased modeling complexity. In particular, because the effective parking capacity available to each vehicle type is no longer fixed and known, we cannot directly apply closed-form Erlang loss results (see Ross (2014), p. 563-564) to evaluate (as in Abhishek et al. (2021)) the societal costs of vehicles' negative externalities. The server pool is now multi-rate, meaning the offered load per server varies across parking spaces due to different demand rates and localized access of logistic vehicles. Additionally, there is no longer a sequential assignment of logistic vehicles to first logistic and then regular parking spaces. Within this setting, we establish a Continuous Time Markov Chain (CTMC) submodel in Section 3.2, which enables us to measure the societal costs of interest.

3.2 A Continuous Time Markov Chain Component

Given a binary parking space reservation $\mathbf{x}$, a state space $\mathcal{S}(\mathbf{x})$ includes all possible occupancy configurations of the parking spaces $\mathcal{I}$ along the street. Each state $s \in \mathcal{S}(\mathbf{x})$ is represented by a vector of length $|\mathcal{I}|$. The i^{th} element of the state variable is conditional on $\mathbf{x}$. Mathematically, $s_i|_{(x_i=1)} \in \{0, 1\}$ and $s_i|_{(x_i=0)} \in \{0, 1, 2\}$, indicates the occupancy status of parking space $i \in \mathcal{I}$, where:

- $s_i = 0 \coloneqq$ the space is vacant,
- $s_i = 1 \coloneqq$ the space is occupied by a logistic vehicle,
- $s_i = 2 \coloneqq$ the space is occupied by a passenger vehicle.

Recall that δ_j, denoting the set of parking spaces accessible to establishment $j \in \mathcal{J}$, is independent of reservation decisions $\mathbf{x}$. In contrast, the set of parking spaces available to passenger vehicles depends on the reservation vector $\mathbf{x}$. This is because if a particular space $i \in \mathcal{I}$ is reserved for logistic vehicles, the corresponding state element s_i can no longer take the value of 2. Therefore, we define $\delta_2(\mathbf{x}) = \{i \in \mathcal{I} \mid x_i = 0\}$ as the set of spaces not reserved for logistics use.

Given a reservation vector $\mathbf{x}$, the set of parking spaces δ_j for delivery to establishment $j \in \mathcal{J}$, and the available parking spaces for passenger vehicles $\delta_2(\mathbf{x})$, we define the following sets, which enable us to track the transition probabilities in the parking configurations of the street upon a vehicle arrival or departure.

- $\mathcal{F}_{1j}(s) = \{i \in \delta_j \mid s_i = 0\} \coloneqq$ Set of free parking spaces in state s available to a logistic vehicle when serving establishment $j \in \mathcal{J}$,
- $\mathcal{F}_2^{\mathbf{x}}(s) = \{i \in \delta_2(\mathbf{x}) \mid s_i = 0\} \coloneqq$ Set of free parking spaces in state s available to passenger vehicles.

Finally, let π_s denote the steady-state probability of state s, and $Q(\mathbf{x})$ the generator matrix of the CTMC for a given solution $\mathbf{x}$. We proceed by constructing all feasible state transitions based on vehicle arrival and departure events, which together define the generator matrix $Q(\mathbf{x})$.

3.2.1 Vehicle Arrivals

Consider a state $s \in \mathcal{S}(\mathbf{x})$ representing the current occupancy configuration of the street. For any establishment $j \in \mathcal{J}$, if there exists at least one free parking space accessible to logistic vehicles, i.e., $|\mathcal{F}_{1j}(s)| \geq 1$, the arrival of a logistic vehicle is accepted and we assume is assigned uniformly at random to one of the parking spaces $i \in \mathcal{F}_{1j}(s)$. Specifically, for each $i \in \mathcal{F}_{1j}(s)$, the transition $s_i : 0 \rightarrow 1$ occurs at rate $\lambda_{1j}/|\mathcal{F}_{1j}(s)|$. Importantly, if the arriving logistic vehicle experiences shortcomings in parking spaces, i.e., $|\mathcal{F}_{1j}(s)| = 0$, its arrival across the transitions is blocked, which represents an illegal parking event while the parking configuration s remains intact.

An analogous structure applies to passenger vehicles. If some vacant general-use parking spaces exist, i.e., $|\mathcal{F}_2^{\mathbf{x}}(s)| \geq 1$, a passenger vehicle arrival is accepted and assigned uniformly among parking spaces $i \in \mathcal{F}_2^{\mathbf{x}}(s)$. Here, for each $i \in \mathcal{F}_2^{\mathbf{x}}(s)$, the transition $s_i : 0 \rightarrow 2$ occurs at rate $\lambda_2/|\mathcal{F}_2^{\mathbf{x}}(s)|$. If $|\mathcal{F}_2^{\mathbf{x}}(s)| = 0$, the arriving passenger vehicle cannot be accommodated on the street and is therefore blocked, and the system

state s remains unchanged. This corresponds to a cruising event, after which the vehicle leaves the street, either spilling over into neighboring streets or diverting to a central parking facility (if available).

3.2.2 Vehicle Departures

The state transitions induced by vehicle departures are comparatively straightforward. If a parking space $i \in \mathcal{I}$ is occupied by a logistic vehicle ($s_i = 1$), it transitions to vacant status ($s_i : 1 \rightarrow 0$) at rate μ_1. Else, if it is occupied by a passenger vehicle ($s_i = 2$), the transition $s_i : 2 \rightarrow 0$ occurs at rate μ_2.

These arrival and departure transitions collectively define the off-diagonal entries of $Q(\mathbf{x})$, with diagonal entries determined as $Q(\mathbf{x})(s, s) = -\sum_{s' \neq s} Q(\mathbf{x})(s, s')$ such that each row of $Q(\mathbf{x})$ sums to zero. Here, the steady-state probabilities of these states serve as continuous decision variables. With that in mind, we derive our objective function in Section 3.3

3.3 Derivation of the objective function

Given a binary reservation vector $\mathbf{x}$ and its associated steady-state probability vector $\pi(\mathbf{x})$, we measure the total negative societal costs $C(\mathbf{x}, \pi(\mathbf{x}))$ by calculating two key performance metrics. Eq. (2a) measures the expected societal cost of illegal parking of logistic vehicles, denoted by Ω_1. It captures the expected cost of total illegal parking events by multiplying the unit societal cost α_1 of an illegal parking by the sum of arrivals times steady-state probabilities of states in which parking spaces accessible for logistic vehicles are occupied upon their arrival to serve establishment $j \in \mathcal{J}$. Moreover, Eq. (2b) computes the expected societal cost of cruising effect by passenger vehicles, denoted by Ω_2. It quantifies the cost of cruising events by multiplying the corresponding unit cost, α_2, by the arrival rate of passenger vehicles blocked from parking along the street. Darendeliler et al. (2026) employ a commercial traffic microsimulation model to quantify these impacts as marginal externality costs arising from traffic delays due to insufficient parking availability. Their findings indicate a pronounced disparity between α_1 and α_2, with $\alpha_1 > \alpha_2$. In particular, α_1 captures the congestion and delay effects of road blockage, which are typically more severe than the less disruptive effects associated with cruising for parking, represented by α_2. Finally, our objective is presented in Eqs. (2) and (3).

$$\Omega_1(\mathbf{x}, \pi(\mathbf{x})) = \sum_{j \in \mathcal{J}} \sum_{\substack{s \in \mathcal{S}: \\ |\mathcal{F}_{1j}(s)|=0}} \lambda_{1j} \pi_s \tag{2a}$$

$$\Omega_2(\mathbf{x}, \pi(\mathbf{x})) = \lambda_2 \sum_{\substack{s \in \mathcal{S}: \\ |\mathcal{F}_2^{\mathbf{x}}(s)|=0}} \pi_s \tag{2b}$$

$$C(\mathbf{x}, \pi(\mathbf{x})) = \alpha_1 \Omega_1(\mathbf{x}, \pi(\mathbf{x})) + \alpha_2 \Omega_2(\mathbf{x}, \pi(\mathbf{x})) \tag{3}$$

3.4 Bi-level Optimization Model

Now, we are in a position to introduce the nonlinear discrete optimization bi-level model (4). The upper-level (leader) model determines the binary reservation decision vector $\mathbf{x}$ which minimizes the objective function

$C(\mathbf{x}, \pi(\mathbf{x}))$, while the lower-level (follower) model solves a system of linear equations arising from the CTMC equilibrium component described in Section 3.2. Once a solution $\mathbf{x}$ is specified at the upper level (4a)-(4b), the corresponding state space $S(\mathbf{x})$, the generator matrix $Q(\mathbf{x})$, and the CTMC probability variables $\pi(\mathbf{x})$ are parametrized and constructed as described in Section 3.2. Subsequently, Equations (4d)-(4f) are solved to obtain $\pi(\mathbf{x})$. Finally, both $\mathbf{x}$ and $\pi(\mathbf{x})$ are fed into the objective function (4a), which yields the exact objective value associated with the reservation vector $\mathbf{x}$.

$$\min_{\mathbf{x}} \quad C\left(\mathbf{x}, \pi^*(\mathbf{x})\right) \tag{4a}$$

$$\text{s.t.} \quad x_i \in \{0,1\} \quad \forall i \in \mathcal{I} \tag{4b}$$

$$\text{where} \qquad \pi^*(\mathbf{x}) \in \arg\min \sum_{s \in \mathcal{S}(\mathbf{x})} \pi_s \tag{4c}$$

$$\text{s.t.} \quad \pi(\mathbf{x})^\top Q(\mathbf{x}) = 0 \tag{4d}$$

$$\sum_{s \in \mathcal{S}(\mathbf{x})} \pi_s = 1 \tag{4e}$$

$$\pi_s \in [0,1] \quad \forall s \in \mathcal{S}(\mathbf{x}) \tag{4f}$$

Next, we present Proposition 3.1, which establishes that the proposed exact model (4) is $\mathcal{NP}$-hard. The polynomial-time reduction from the $\mathcal{NP}$-complete Subset-Sum problem is provided in the E-Companion. We then elaborate on the problem size and computational complexity in Remark 3.1, which together motivate the methodological developments in Section 4.

Proposition 3.1 *The bilevel SOPP model (4) is $\mathcal{NP}$-hard.*

Remark 3.1 *State-space growth and the necessity of a bilevel model. The construction in the proof of Proposition 3.1 (reduction from the $\mathcal{NP}$-complete Subset-Sum problem) uses only $n+1$ CTMC states, yet in many practical follower models, as in model (4), the state space depends on combinatorial features of $\mathbf{x}$. This causes the follower state space to grow exponentially with the dimension of $\mathbf{x}$. Moreover, in our case, the state space $\mathcal{S}(\mathbf{x})$ and the generator matrix $Q(\mathbf{x})$ both depend on the chosen binary vector $\mathbf{x}$, so the mapping $\mathbf{x} \mapsto \pi(\mathbf{x})$ is* implicitly *defined by a linear system whose coefficients change with $\mathbf{x}$, which entails the derivation of a bilevel model.*

The computational hardness stems from the discrete upper-level choice coupled with the decision-dependent and exponentially-growing steady-state follower response. More specific to model (4), the occupancy state can take one of three possible values, $s_i \in \{0,1,2\}$, whereas a reserved parking space is restricted to two possible states, $s_i \in \{0,1\}$, as passenger vehicles are prohibited from occupying these spaces. Thus, in the worst case, $2^{|\mathcal{I}|}$ possible reservation decisions need to be evaluated, for each of which, the total number of feasible parking configuration states is $|\mathcal{S}(\mathbf{x})| = 3^{|\mathcal{I}|-\mathbf{1}^\top\mathbf{x}} \cdot 2^{\mathbf{1}^\top\mathbf{x}}$.

A natural question that may arise concerns whether to impose an upper bound on the number of reservations. We do not introduce such a bound, practically because there is no clear or justifiable upper

limit that could be imposed a priori. By omitting this restriction, we can observe the model's generic behavior under various reservation configurations and traffic intensities along a street.

3.5 Monotonicity Properties of the Cost Terms

Theorem 3.1 investigates the monotonicity properties in $\mathbf{1}^\top\mathbf{x}$ of the cost terms $\Omega_1(\mathbf{x}, \pi(\mathbf{x}))$ and $\Omega_2(\mathbf{x}, \pi(\mathbf{x}))$ given in Eqs. (2a) and (2b).

Theorem 3.1 *The following characteristics hold:*

- $\Omega_2(\mathbf{x}, \pi(\mathbf{x}))$ *is non-decreasing in* $\mathbf{1}^\top\mathbf{x}$.
- $\Omega_1(\mathbf{x}, \pi(\mathbf{x}))$ *is not monotone in* $\mathbf{1}^\top\mathbf{x}$.

Proof. As established in Corollary 1 of Abhishek et al. (2021), reducing the service capacity (the parking bay area in OPP) available to a customer class strictly increases that class's blocking probability. Given passenger vehicles' street-wide access to all unreserved spaces, this remains valid for SOPP. An increase in the total number of reserved spaces, ($\mathbf{1}^\top\mathbf{x}$), reduces the residual curbside capacity available to passenger vehicles. This translates into a higher blocking probability for passenger vehicles. Hence, the monotonicity of Ω_2 with respect to reservation count follows. In contrast, this argument does not extend to logistic vehicles in SOPP. Their access is spatially localized and tied to establishments with heterogeneous freight demand, so increasing reservations may alter both the spatial distribution of capacity and the matching between demand and supply. We demonstrate the non-monotonicity of Ω_1 via a counterexample provided in the illustrative example in the E-Companion. □

The non-monotonic behavior of Ω_1 in the reservation count precludes the application of finite-step additive/add-drop heuristics (in the spirit of Abhishek et al. (2021)). In the next section, we present a scalable and computationally efficient framework tailored to this structural challenge.

4 Surrogate Modeling

The model (4) at hand involves a complex objective function (3) and an exponentially growing number of decision variables and CTMC balance equations. To address these challenges and design a scalable solution algorithm, we develop a machine learning (ML) based surrogate model that is representative of Eq. (4a) and inherently reflects the CTMC relationships. Specifically, throughout a three-step process, we (i) run Discrete Event Simulation (DES) within a systematic *data farming* framework to generate a sufficiently rich and representative training set. Accordingly, (ii) we establish and train a tractable, closed-form surrogate for the objective function (4a) and (iii) finally solve the problem by replacing the complicating objective function with a computationally tractable ML surrogate.

4.1 Data Farming

We implement a *data-farming phase* to generate the data for training our ML surrogate. Specifically, we run a DES repeatedly across many different reservation vectors to generate data that will later be used to

train and evaluate our models. The DES replicates the stochastic dynamics of parking spaces along a street under both Markovian and non-Markovian assumptions, for any given reservation vector $\mathbf{x}$ and parameter configuration $\Gamma = (\lambda_1, \lambda_{1j}, \lambda_2, \mu_1, \mu_2, \overline{d}, \delta_j)$.

Data farming begins by populating a satisfactory set of reservation vectors, $\mathbf{x}$. For a fixed number of reservations m, there exist $\binom{|\mathcal{I}|}{m}$ distinct reservation vectors over the set of parking spaces $\mathcal{I}$. Let N denote the total number of samples to be generated and stored in the dataset $\mathcal{D}$. At each iteration $n \in N$, we first draw a random integer m from a binomial distribution with parameters (N, η), where $\eta \in (0, 1)$ represents the probability parameter and determines the expected reservation level ηN. Conditioning on m, we then select m distinct parking spaces at random from $\mathcal{I}$. Repeating this procedure N times populates the search space and yields a dataset that is both *pervasive*, in the sense that it broadly spans the reservation space, and *balanced* with respect to coverage across different reservation counts.

Subsequently, for each sampled reservation vector $\mathbf{x}$, we calculate the resulting cost with DES, which we later use to train the ML surrogate. To this end, we replicate a DES of configuration Γ for $r \in \mathbb{Z}^+$ times. The planning horizon of each DES replication is $H \in \mathbb{Z}^+$ hours. Because the problem addresses steady-state peak hours, the DES begins with a fully occupied street. During the interval H, all arrival and departure events of logistic and passenger vehicles are simulated according to the procedures described in Section 3.2. Upon completion of each DES replication, the original objective function (3) is estimated by Equation (5), which averages across replications and the horizon length.

$$\overline{C}(\mathbf{x_n}) \;=\; \frac{\alpha_1 \psi_1(\mathbf{x_n}) + \alpha_2 \psi_2(\mathbf{x_n})}{rH}, \tag{5}$$

where ψ_1 and ψ_2 denote the total number of blocked parking events accumulated for logistic and passenger vehicles, respectively, across all replications. Specifically, ψ_1 increases whenever a logistic vehicle arrival at establishment $j \in \mathcal{J}$ cannot be accommodated within its designated δ_j parking spaces, and ψ_2 increases whenever a passenger vehicle arrives and the parking spaces designated for passenger use (i.e., those with $x_i = 0$) are all occupied. A key advantage of the DES framework for cost calculation, in contrast to the CTMC model (4), is that it does not rely on Markovian assumptions and can therefore accommodate general interarrival and service time distributions, if necessary.

After constructing the feature dataset $\mathcal{D}$ and its associated performance estimates $\overline{C}(\mathbf{x})$, we partition $\mathcal{D}$ into training and test subsets.

Remark 4.1 *The unbiasedness of the estimator in Equation* (5) *requires only mild conditions: (i) the r replications are* i.i.d.*, (ii) each replication is generated by the same DES mechanism governed by the primitives specified in the parameter configuration* Γ*, and (iii) the underlying random variables admit finite first moments.*

4.2 ML Surrogate

The binary decision variables x_i associated with parking spaces $i \in \mathcal{I}$ exhibit neighborhood-based interactions. This local coupling structure is characteristic of systems in which each decision variable both

influences and is influenced by its neighbors, as commonly observed in image processing, spatial statistics, and graph-based optimization problems. Accordingly, using the training dataset, we fit a closed-form *Quadratic Boolean function*, denoted by $g(\mathbf{x})$, as defined in Equation (6). The parameters of this surrogate are obtained via Ridge regression (i.e., L_2-regularized least squares), which mitigates multicollinearity and prevents overfitting by penalizing the squared magnitude of the coefficients. This method can be interpreted as the maximum a posteriori estimator of $\boldsymbol{\beta}$ under a Gaussian prior on the coefficients. The coefficient vector is thus computed as $\boldsymbol{\beta} = (\Phi^\top \Phi + \gamma I)^{-1}.\Phi^\top \mathbf{y}$ where Φ denotes the feature matrix containing the linear and quadratic terms, $\gamma = 1$ is the regularization parameter, I is the identity matrix of appropriate dimension, and $\mathbf{y}$ is the response vector consisting of the DES observed costs $\overline{C}$.

$$g(\mathbf{x}) = \beta_0 + \sum_{i \in \mathcal{I}} \beta_i x_i + \sum_{i,i' \in \mathcal{K}} \beta_{ii'} x_i x_{i'} \tag{6}$$

The surrogate (6) properly models the neighborhood-based interactions and provides a computationally tractable yet expressive approximation of the complex objective function in Equation (3). The quadratic terms $x_i x_{i'}$ in Equation (6) may be defined for all $i, i' \in \mathcal{I}$ with $i < i'$. However, such a formulation induces strong dependence between the linear and quadratic coefficients, which adversely affects training precision, particularly in SOPP instances with long streets. To improve tractability, we restrict the quadratic interactions to pairs of parking spaces $(i, i') \in \mathcal{K}$ where $\mathcal{K}$ denotes the set of tuples of parking spaces that serve at least one common establishment, i.e., $\mathcal{K} = \left\{(i, i') \in \mathcal{I} \times \mathcal{I} : i < i' \wedge \exists\, j \in \mathcal{J} : i, i' \in \delta_j\right\}$.

Equation (6) represents a Quadratic Unconstrained Binary Optimization (QUBO) problem, which is a canonical form for optimization over binary variables with quadratic interactions. In this formulation, the decision vector $\mathbf{x} \in \{0, 1\}^{\mathcal{I}}$ directly encodes reservation assignments, and the quadratic terms $\beta_{ii'} x_i x_{i'}$ capture neighborhood-based interactions between parking spaces. QUBO problems are widely studied in combinatorial optimization because they can compactly encode local and pairwise dependencies while remaining unconstrained, aside from the binary restrictions. One natural approach to solving the QUBO in Equation (6) is to treat it as a mixed-integer nonlinear programming (MINLP) problem, where the binary variables are explicitly enforced, and the quadratic objective is optimized directly. Given the typical problem sizes encountered in practice, commercial MINLP solvers such as CPLEX or Gurobi can efficiently solve the surrogate model $g(\mathbf{x})$ to optimality.

5 Computational Experiments

In Section 5.1, we construct a real-world test case based on Şehit Mithat Yılmaz (SMY) Street (Figure 2), a traffic-intensive corridor in the Sarıyer district of Istanbul, where curb space demand from both logistic and passenger vehicles is high. Section 5.2 presents the computational results for the baseline instance, including run times, solution quality, and comparative evaluations of the proposed solution methods.

(a) A publicly-available photo (https://yandex.com.tr/)

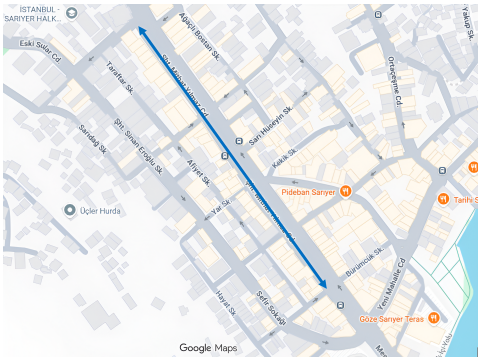

(b) Area of study, shown with the arrowed line (https://maps.google.com/)

Figure 2: Our case study "Şehit Mithat Yılmaz Caddesi" street in Istanbul

5.1 Test Case Design

Designing an instance of our problem requires quantifying *ten* key parameters, which we detail below and list their values in Table 3. The parametrization of the first nine elements, including the arrival and parking rates for the passenger and logistic vehicles, is borrowed from the traffic analysis outputs of Darendeliler et al. (2026).

- **Set of parking spaces** ($\mathcal{I}$): The study area, SMY Street (see Figure 2b), extends approximately 400 meters in length. Owing to the approximate symmetry between the two traffic directions, we restrict our analysis to a single direction. After excluding designated bus stops and taxi stands, 47 curbside parking spaces remain available for consideration in the computational experiments. Accordingly, we define the index set of parking spaces as $\mathcal{I} = \{1, 2, \cdots, 47\}$.

- **Set of delivery buildings** ($\mathcal{J}$): We identified 35 near-street commercial establishments as delivery addresses for logistic vehicles along the study area of SMY street, as shown in Figure 2b. Accordingly, we define the set of commercial establishment as $\mathcal{J} = \{1, 2, \cdots, 35\}$.

- **Distance matrix** ($d_{ij}\ \forall i \in \mathcal{I}, j \in \mathcal{J}$): We collected the latitude and longitude coordinates for all nodes in sets $\mathcal{I}$ and $\mathcal{J}$. Since d_{ij} represents the walking distance for the logistic vehicle driver, we compute the symmetric Euclidean distance (in meters) between each i–j pair.

- **Arrival rate of logistic vehicles** ($\lambda_{1j}\ \forall j \in \mathcal{J}$): The arrival rate of logistic vehicles λ_1 is set to $0.07m$ vehicles per hour, where m equals the number of parking spaces. In our case, this parameter can be set to $0.07 \times 47 = 3.29$ vehicles per hour on the SMY street. Notably, determining the exact arrival rate for each establishment λ_{1j} is not trivial. As a practical solution, delivery locations can be categorized based on their demand for logistics services, and a ranking system can be used to estimate these rates. Since our goal is to understand how reservation decisions behave under different λ_{1j} values rather than focusing on a single estimate, we distribute λ_1 across the 35 establishment under three scenarios: (i) randomly generated values, (ii) identical and evenly distributed values, and (iii) values increasing

in a structured order. This approach allows us to capture a range of arrival conditions. We further elaborate on these scenarios in Section 5.2.

- **Arrival rate of passenger vehicles** (λ_2): The arrival rate of passenger vehicles λ_2 is set to $0.74m$ vehicles per hour, where m equals the number of parking spaces. In our case, this parameter can be set to $0.74 \times 47 = 34.78$ vehicles per hour on the SMY street.

- **Parking rate of logistic vehicles** (μ_1): This parameter is set to 1.97 vehicles per hour.

- **Parking rate of passenger vehicles** (μ_2): Darendeliler et al. (2026)'s case study suggests passenger parking times follow a two-phase Coxian distribution with independent exponential phases with rates $\tilde{\mu}_p^1 = 0.82$ and $\tilde{\mu}_p^2 = 8.16$ vehicles per hour. In their setting, after the first phase, the process proceeds to the second phase with probability $p = 0.83$; otherwise, it ends. Thus, to obtain an average parameter μ_2 for various distributions, we measure μ_2 as in Equation (7).

$$\mu_2 = \left(\frac{1}{0.82} + 0.83.\frac{1}{8.16}\right)^{-1} = 0.76 \quad \text{vehicles per hour} \tag{7}$$

- **Marginal Externality costs** (α_1, α_2): In our setting, due to the linear structure of the objective function, the relative magnitude of α_1 and α_2 is more consequential than their absolute values. We adopt a baseline ratio of $\alpha_1/\alpha_2 = 4$, which we deem more realistic for the problem context, and subsequently examine the sensitivity of our results to alternative ratios. Accordingly, we set $\alpha_1 = 4$ and $\alpha_2 = 1$.

- **Last-mile delivery threshold** $\left(\overline{d}\right)$: Given that most businesses along the street (white goods sellers, supermarkets, and restaurants) receive their replenishments typically in large payloads, we set $\overline{d} = 40$ meters.

- **DES parameters** N, r, H, η: Since the busy period on SMY Street extends throughout the daytime, we set $H = 8$ hours. Given the much lower arrival rate of delivery vehicles relative to passenger vehicles and their shorter parking durations, we set $\eta = 0.1$.

  To determine the number of generated data points (N) and the number of simulation runs per allocation alternative (r), we tested several configurations, as reported in Table 2, which summarizes the prediction accuracy of the ML model in the test set in terms of the coefficient of determination (R^2). Targeting $R^2 \geq 0.95$, we set $N = 10{,}000$ and $r = 1{,}000$. Larger values were not considered, as they would substantially increase the computational burden of the DES while yielding only marginal improvements in accuracy.

5.2 Numerical Results

In this section, we implement the proposed three-step solution framework, comprising data farming, surrogate modeling, and surrogate-based optimization, on the test instance described in Section 5.1. The framework is

Table 2: Average test-set R^2 performance of the data-farming across the three scenarios for multiple N and r configurations.

	r				
N	200	400	600	800	1000
2000	0.81	0.88	0.90	0.91	0.92
4000	0.84	0.89	0.92	0.93	0.93
6000	0.85	0.90	0.92	0.93	0.94
8000	0.86	0.91	0.93	0.94	0.94
10000	0.86	0.91	0.93	0.94	0.95

Table 3: Test case parameter design

Definition	Notation	Value
Set of parking spaces	$\mathcal{I}$	$\{1, 2, \cdots, 47\}$
Set of delivery buildings	$\mathcal{J}$	$\{1, 2, \cdots, 35\}$
Distance matrix	$d_{ij}\ \forall i \in \mathcal{I}, j \in \mathcal{J}$	See Table EC.5 in the E-Companion
Arrival rate of logistic vehicles	λ_1	3.29 vehicles per hour. For $\lambda_{1j}\ \forall j \in \mathcal{J}$ of scenario 1, see Table EC.6 in the E-Companion
Arrival rate of passenger vehicles	λ_2	34.78 vehicles per hour
Parking rate of logistic vehicles	μ_1	1.97 vehicles per hour
Parking rate of passenger vehicles	μ_2	0.76 vehicles per hour
Marginal Externality costs	(α_1, α_2)	(4, 1)
Last-mile delivery threshold	$\overline{d}$	40 meters
DES parameters	(N, r, H, η)	(10000, 1000, 8, 0.1)

coded in Python, with the surrogate function modeled using the Pyomo library and solved via the GUROBI 12.0.1 SolverFactory, on a laptop with an Intel(R) Core(TM) i7 3.00GHz CPU and 16 GB RAM. The data farming step is conducted in parallel across 12 cores, lasting around 3 hours on the system under the provided (N, r, H, η) configuration in Table 3. The next two steps, i.e., surrogate modeling and solving it, take place in the order of seconds, so we forgo reporting their run times.

Using the average logistic vehicle arrival rate $\lambda_1 = 3.29$, we construct three demand scenarios to evaluate the performance of the reservation policies. In Scenario 1, the arrival rates λ_{1j} for delivery establishments $j \in \mathcal{J}$ reflect a heterogeneous distribution as illustrated in Figure 3. Scenarios 2 and 3 are designed to provide additional structural insights into the behavior of the proposed methods. In Scenario 2, demand is uniformly distributed across establishments, with identical arrival rates $\lambda_{1j} = 0.094\ \forall j \in \mathcal{J}$ vehicles per hour. In Scenario 3, arrival rates decrease linearly with the establishments index, specifically, $\lambda_{1j} = 0.148 - 0.003j,\ \forall j \in \mathcal{J}$.

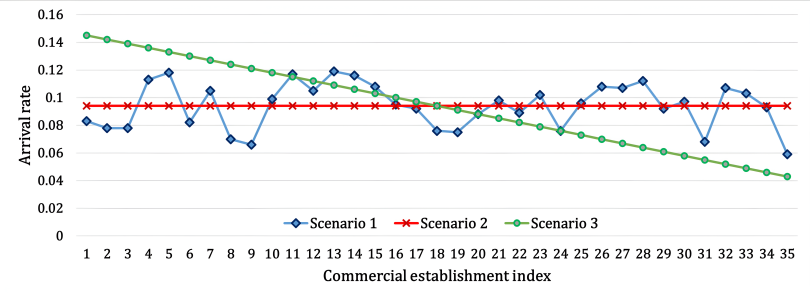

Figure 3: logistic vehicle arrival patterns in Scenarios 1 (heterogeneous arrival rates), 2 (uniform arrival rates of 0.094 vehicles per hour), and 3 (linearly decreasing arrival rates).

For each of the three scenarios, we solved the corresponding surrogate function. Table 4 reports the

resulting optimal parking reservation plans, the total number of reserved spaces, the optimal surrogate objective value $g(\mathbf{x}^*)$ as hourly incurred cost externalities, and the corresponding performance estimate $\overline{C}(\mathbf{x}^*)$ obtained by evaluating $\mathbf{x}^*$ via DES. We also report the relative estimation gap, computed as $100 \times (\overline{C}(\mathbf{x}^*) - g(\mathbf{x}^*))/\overline{C}(\mathbf{x}^*)$, to assess the accuracy of the surrogate model. The small percentage gaps indicate that the surrogate function is well calibrated.

Table 4: Optimal results for our test case instances

Scenario	Optimal reservation $\mathbf{x}^* : (x_i = 1)$	Total reserved $(\mathbf{1}^\top \mathbf{x})$	Surrogate objective value $g(\mathbf{x}^*)$ in Eq. (6)	DES result $\overline{C}(\mathbf{x}^*)$ using Eq. (5)	Estimation gap %
1	[7, 18, 24, 27, 37]	5	8.555	8.569	0.163
2	[7, 24, 27, 40]	4	8.558	8.636	0.903
3	[7, 9, 19, 24, 27]	5	8.330	8.544	2.505

5.3 Best responses for given total reservations

To examine how the objective function varies with the total number of reservations, we impose the additional constraint $\sum_{i \in \mathcal{I}} x_i = k$ when solving the surrogate model $g(\mathbf{x})$. We then resolve the model for different values of k over the range $\{0, 1, \cdots, 20\}$. The resulting objective values for the three scenarios are presented in Figure 4. In this figure, the best total reserved value is highlighted as a larger red point, aligned with the results of Table 4. The presence of interior minima, rather than only at the extreme cases where the total number of reservations is 0 or $\mathcal{I}$, is consistent with the counterintuitive findings reported by Abhishek et al. (2021). The authors describe two opposing effects: *space reduction* and *competition reduction*. The former is straightforward, as reserving spaces reduces the capacity available to passenger cars. The latter, however, suggests that allocating spaces to logistics bays does not necessarily worsen service levels for cars and may even reduce their blocking probability. Although dedicating space to logistic vehicles limits car capacity, it also reduces the need for them to compete for regular parking spaces. Consequently, up to some reservation levels, the competition-reduction effect dominates the space-reduction effect. Beyond a certain point, this balance reverses, revealing a trade-off between the two mechanisms.

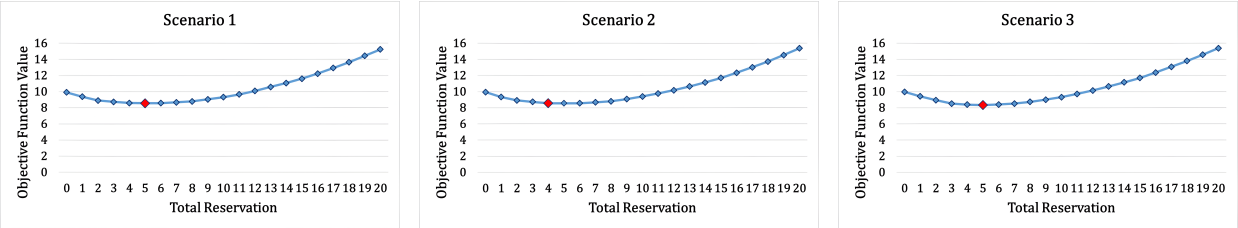

Figure 4: Optimal objective function values for given different total reservation numbers

Finally, Table 5 reports the optimal reservation vectors $\mathbf{x}^*$ with $x_i = 1$ for total reservation levels $k \in \{1, 2, \cdots, 10\}$. Notably, and consistent with the discussion in Section 3.5, the solutions do not follow a simple additive (greedy) pattern. In particular, as k increases, the solution for $k + 1$ reservations does not necessarily build on the solution for k reservations when a single reservation is added. This indicates non-monotonic and non-nested behavior in the optimal reservations.

Table 5: Optimal reservation solution $\mathbf{x}^*$ for different total reservation counts

k	Reserved parking spaces $\mathbf{x}^*$: $x_i = 1$		
	Scenario 1	Scenario 2	Scenario 3
1	[24]	[25]	[24]
2	[24, 27]	[24, 27]	[7, 24]
3	[24, 27, 37]	[7, 24, 27]	[7, 24, 27]
4	[7, 24, 27, 37]	[7, 24, 27, 40]	[7, 17, 24, 27]
5	[7, 18, 24, 27, 37]	[7, 24, 27, 28, 40]	[7, 9, 19, 24, 27]
6	[7, 18, 24, 27, 28, 40]	[7, 18, 24, 27, 28, 40]	[7, 9, 19, 23, 25, 26]
7	[7, 17, 23, 25, 26, 36, 41]	[7, 18, 24, 27, 28, 37, 40]	[7, 9, 19, 23, 25, 26, 36]
8	[7, 12, 21, 23, 25, 26, 36, 41]	[7, 9, 19, 23, 25, 26, 36, 40]	[2, 9, 12, 19, 23, 25, 26, 36]
9	[7, 12, 21, 23, 25, 28, 30, 39, 40]	[7, 9, 19, 23, 25, 27, 33, 41, 44]	[2, 9, 12, 19, 23, 25, 26, 36, 40]
10	[2, 9, 12, 21, 23, 25, 28, 30, 39, 40]	[7, 10, 16, 23, 24, 25, 27, 33, 41, 44]	[2, 9, 12, 19, 21, 23, 25, 26, 36, 40]

5.4 Cross-Validation

To further validate our proposed framework against established results in the literature, we replicate the setting of "Example 2: Passenger-Intensive Area" from Section 6.2 of Abhishek et al. (2021). This example is particularly suitable for validation, as its arrival and service characteristics closely resemble realistic on-street parking environments. To match this configuration with our framework, we adopt the following parameterization and coding adjustments:

- The total parking capacity in the original example is 20 spaces. Accordingly, we set $|\mathcal{I}| = 20$ and consider a single establishment $|\mathcal{J}| = 1$.
- All pairwise distances are set to one, and the walking-distance threshold is also set to one. This relaxes spatial restrictions and allows logistic vehicle drivers to park at any location along the street, consistent with the benchmark's assumptions.
- To reflect the sequential search behavior described in Abhishek et al. (2021), we modify our DES logic so that logistic vehicles first attempt to occupy reserved logistics bays (i.e., spaces with $x_i = 1$). Only if no reserved space is available do they search for a passenger space (i.e., $x_i = 0$). This enforces the same priority structure as in the original model.
- Arrival and service parameters follow the benchmark specification, converted to hourly rates: $\lambda_1 = 24, \mu_1 = 2$ (logistic), $\lambda_2 = 48, \mu_2 \in \{1, 1.5, 2\}$ (passenger).
- For each reservation level $\mathbf{1}^\top \mathbf{x} \in \{0, 1, \ldots, 20\}$, we run the DES once for the corresponding number of reserved spaces. Because locations are homogeneous in this benchmark, only the count of reserved spaces (not their specific positions) affects performance. For each configuration, we conduct $r = 1000$ replications over a simulation horizon of $H = 8$ hours.
- Although multiple performance metrics can be evaluated, we focus on blocking probability, as it directly aligns with our objective function, making it the most relevant measure for benchmarking system performance. Blocked vehicle counts are obtained directly from $\psi_1(\mathbf{x})$ and $\psi_2(\mathbf{x})$ defined in Equation (5). Following Abhishek et al. (2021), we compute the blocking probabilities for logistic and passenger vehicles as

$$B_1(\mathbf{x}) = \frac{\psi_1(\mathbf{x})}{rH\lambda_1}, \qquad B_2(\mathbf{x}) = \frac{\psi_2(\mathbf{x})}{rH\lambda_2}. \tag{8}$$

Figure 5 reports the resulting blocking probabilities $B_1(\mathbf{x})$ and $B_2(\mathbf{x})$ for reservation levels $\mathbf{1}^\top\mathbf{x} \in \{0, 1, \ldots, 20\}$. The observed trends closely replicate those shown in Figures 4(a)–(b) of Abhishek et al. (2021). This benchmarking exercise provides external validation of the proposed framework and supports its use for the more extensive sensitivity analyses and managerial insights developed in Section 6.

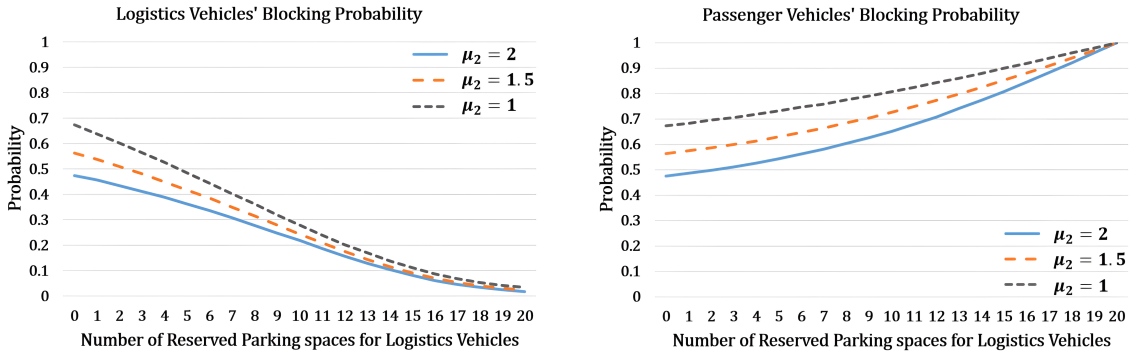

Figure 5: Blocking probabilities of logistic and passenger vehicles benchmarked with the "Example 2: Passenger-Intensive Area" from Section 6.2 of Abhishek et al. (2021).

6 Sensitivity Analysis and Managerial Insights

Throughout Section 6, we investigate the OPP problem and derive managerial insights. In Section 6.1, we quantify the benefits of our proposed framework relative to existing aggregate models and heuristic approaches. In Section 6.2, we conduct one-way sensitivity analysis to examine the impact of key parameters on reservation decisions and overall costs. Section 6.3 extends the model to a cross-parking regime, in which logistic vehicle drivers can park on either side of the street for delivery.

6.1 Benefit of Location-Aware Reservation Decisions

In this section, we motivate the development of our optimization framework for SOPP by comparing it with two alternative decision-making approaches: a location-ignorant planning policy and two reservation heuristics that differ in their level of sophistication and computational effort.

In the `location-ignorant` policy, we adopt the state-of-the-art OPP approach described in Abhishek et al. (2021) by relaxing the walking distance threshold for deliveries and imposing a sequential flow in which logistic vehicle arrivals first attempt to park in reserved bays and, if these are full, spill over to shared spaces. We observe that this method substantially reduces the number of reservations allocated to logistic vehicles and underestimates the external costs associated with illegal parking (see also Subsection 6.2.3 for analysis on $\overline{d}$). In our baseline test case, the location-ignorant approach resulted in zero reserved parking spaces—mirroring the current no-reservation practice—whereas SOPP recommended reserving five spaces for logistic vehicles. This policy exhibited a performance gap of approximately 15% relative to the proposed method; under traffic-intensive conditions, the gap exceeded 30%, indicating that such simplifications become increasingly misleading as congestion intensifies. Importantly, location-ignorant planning not only neglects

the spatial placement of reservations but may also recommend a different number of reserved spaces. This observation suggests that determining the number of reservations using existing OPP-type approaches and subsequently selecting their locations may fail to produce high-quality solutions.

For the heuristic reservation policy benchmarks, we first determine a reasonable bound, $\bar{n}$, for the number of reservations to consider, and then for each $n \in \{1, \ldots, \bar{n}\}$ we distribute them spatially using heuristic rules and report the best-performing solution. In our tests, we used $\bar{n} = 10$ for the heuristics, as increasing the reservations beyond this number cannot yield high-quality solutions in our case, while significantly increasing the computational effort.

We evaluate two heuristic strategies. The first is a stratified `naïve scatter` policy. For a given total number of reservations n, the street is partitioned into n equal segments, and one parking space is randomly selected from each segment to ensure an even spatial distribution. The resulting reservation vector is evaluated using DES. For each $n \in \{1, \ldots, \bar{n}\}$, we explore 100 random configurations $\mathbf{x}$ and report the best-performing outcome across all values of n in Table 6.

The second heuristic adopts a more structured approach based on a variant of the `Maximum Covering Problem (MCP)`, formulated as model (9). For a fixed reservation budget n, spaces are selected to maximize the number of nearby commercial establishments effectively served. Coverage is demand-weighted: each establishment is assigned a weight proportional to the offered load it generates per allocated parking space, computed via a knapsack-style ratio as in Eq. (9a). Moreover, weights increase concavely to reflect diminishing marginal benefits, consistent with the behavior of blocking probabilities as capacity grows. We note that this heuristic does not explicitly model blocking probabilities; instead, the concavity parameter κ serves as a proxy. Although the `MCP` formulation is nonlinear due to the concave objective in Eq. (9a), we solve an equivalent linearized MIP formulation (provided in the E-Companion). For each combination of n and κ, we solve `MCP`(n, κ), evaluate the resulting reservation vector $\mathbf{x}$ via DES, and report the best-performing combo in Table 6.

$$\texttt{MCP(n,}\kappa\texttt{)} \quad \max \sum_{j \in \mathcal{J}} \frac{\lambda_{1j}}{|\delta_j|} \cdot \left(\sum_{i \in \delta_j} x_i \right)^{\kappa} \tag{9a}$$

$$\text{S.t.} \sum_{i \in \mathcal{I}} x_i \leq n \tag{9b}$$

To facilitate a more informative comparison among the SOPP, `location-ignorant` policy, `Naïve Scatter` policy, and `MCP` policy, we analyze two instances. The first corresponds to the baseline test case introduced in Section 5.1. The second represents a higher-traffic variant of this baseline. Specifically, passenger arrival rates are multiplied by 1.5, and logistic vehicles' arrival rates are doubled, while all other parameters remain unchanged. The % estimation gap values are measured by $100 \times$ (Cost value $- g(\mathbf{x}^*)) / g(\mathbf{x}^*)$.

Based on our `MCP` experiments, Remark 6.1 highlights the role of κ in balancing dispersion and concen-

Table 6: Performance comparison of our model with two heuristic policies over the baseline test case instance (1) and a traffic-intensive instance (2)

Instance	SOPP		Location-ignorant policy			Naïve Scatter policy			MCP policy			
	$g(\mathbf{x}^*)$	$\mathbf{1}^\top\mathbf{x}$	$g(\mathbf{x}^*)$	$\mathbf{1}^\top\mathbf{x}$	% Gap	$\overline{C}(\mathbf{x})$	$\mathbf{1}^\top\mathbf{x}$	% Gap	$\overline{C}(\mathbf{x})$	$\mathbf{1}^\top\mathbf{x}$	κ	% Gap
1	8.555	5	9.912	0	15.86	9.345	5	9.23	8.840	5	0.6	3.33
2	28.086	11	37.752	0	34.42	30.620	10	9.02	30.023	10	0.1	6.90

tration in the reservation spaces $\mathbf{x}$.

Remark 6.1 *In the MCP policy, lower values of κ lead to a more dispersed allocation of reservation spaces, promoting spatial spread across the network. As κ increases, the policy gradually shifts its emphasis from dispersion toward concentration by prioritizing locations near establishments with higher knapsack-based weights. Consequently, a proper value of κ trades off a stronger preference for demand intensity and spatial coverage.*

Insight 1. *In terms of objective function values, the proposed method consistently outperforms the benchmark policies, with the ranking: SOPP > MCP Policy > Naïve Scatter Policy > Location-ignorant Policy. The results demonstrate that spatial allocation plays a key role in system performance. Our method jointly optimizes the reservation count and its spatial placement in a dynamic environment with various arrival rates and parking accessibility. Furthermore, the relative performance gains of our model increase under traffic-intensive scenarios. This indicates that spatially informed reservation design becomes even more necessary as congestion intensifies.*

Insight 2. *Regarding the MCP policy, we observe that the concavity parameter κ decreases in high-intensity settings. This suggests that, under congested conditions, broader spatial coverage becomes more important than concentrating capacity around establishments $j \in \mathcal{J}$ with high knapsack ratios of $\lambda_{1j}/|\delta_j|$.*

6.2 Effects of System Parameters on Reservations and Total Costs

6.2.1 Arrival and Departure Rate Analysis

In this section, we perform a one-way sensitivity analysis to examine the impact of logistic vehicle arrival and departure rates on the objective function value and the total number of reserved spaces, using the baseline test case under Scenario 1. Specifically, we scale the arrival rates λ_{1j} for all $j \in \mathcal{J}$ and the service rate μ_1 by a multiplier drawn from the set $\{0.5, 0.75, 1, 1.25, 1.5, 1.75, 2\}$. The results are presented in Figure 6. Figure 6a indicates that both the objective function value and the total number of reservations increase almost linearly with the arrival rates of logistic vehicles. This suggests a near-linear relationship between illegal parking incidents (or blocking events) and demand intensity. In contrast, Figure 6b shows that increasing the departure rate (i.e., reducing average parking duration) leads to a decline in both performance indicators. However, the marginal improvement diminishes as the service rate increases, eventually approaching a plateau.

Insight 3. *System performance is more sensitive to increases in logistic vehicles' arrival rates than to reductions in their parking duration. This indicates that demand pressure, rather than parking duration, is*

the dominant driver of congestion and illegal parking in environments where curb space is shared between logistic and passenger vehicles and is largely occupied by passenger vehicles. The shared, and passenger-dominated curb space is a defining characteristic of our setting, unlike existing studies that assume segregated parking bays for logistic and passenger vehicles.

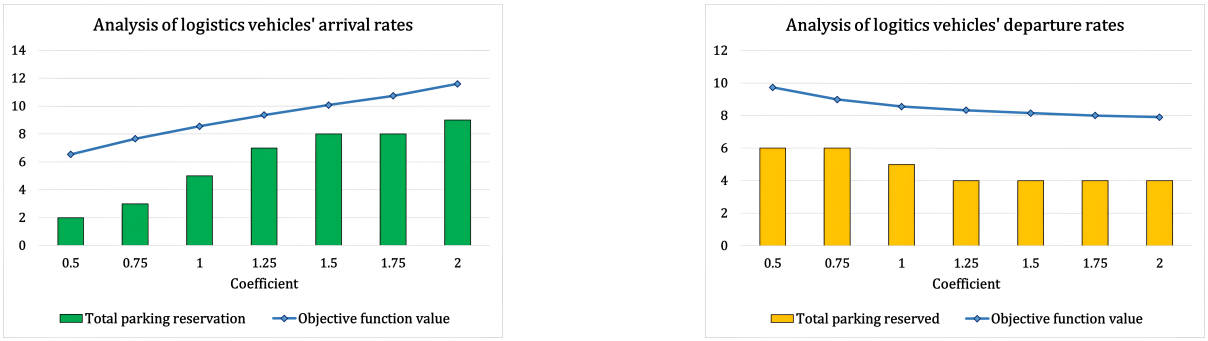

(a) (b)

Figure 6: Effect of varying arrival and departure rates of logistic vehicles on the surrogate objective function value and total parking reservation

6.2.2 Objective Function Cost Terms Analysis

In this analysis, we investigate the impact of varying the penalty associated with blocked (illegal) parking of logistic vehicles on both the objective function value and the total number of reserved parking spaces. Specifically, we set $\alpha_1 \in \{2, 3, 4, 5, 6, 7, 8\}$ while fixing $\alpha_2 = 1$, where $\alpha_1 = 4$ corresponds to the baseline test case. As illustrated in Figure 7, both performance indicators exhibit a concave response to increases in α_1. While the objective function value increases at a decreasing rate, the total number of reservations stabilizes once $\alpha_1 \geq 5$, at which point the model yields identical reservation counts and even identical spatial reservation configurations. This indicates that the solution structure becomes insensitive to further increases in the logistic vehicles' blocking penalty.

Insight 4. *The system is sensitive to the relative penalty of logistic vehicles' blocking events primarily within the range* $\alpha_1/\alpha_2 \in [0, 5]$. *Beyond this threshold, increasing the cost of illegal logistic vehicles' parking does not induce additional reservations or alter the spatial configuration; it only increases the magnitude of the objective function value. This saturation effect, stemming from the underlying queuing model, suggests that, under fixed arrival-departure conditions, there exists a structural upper bound on the amount of curb space that can be allocated to logistic vehicles.*

6.2.3 Walking Distance Threshold Analysis

In this section, we examine the impact of the walking distance threshold on the total number of parking reservations and the surrogate objective value. Specifically, we vary the maximum walking distance as $\overline{d} \in \{30, 40, \ldots, 100\}$ meters, where the feasible parking sets δ_j, $j \in \mathcal{J}$, are defined according to Eq. (1). An increase in $\overline{d}$ enlarges the feasible parking set for each commercial establishment. It allows

logistic vehicles to access more parking spaces. This effectively reduces spatial competition among delivery vehicles, alleviates pressure on high-demand streets, and consequently decreases the incidence of illegal parking. Unlike regulatory parameters, $\overline{d}$ is behavior-driven: it depends on drivers' willingness to walk, street safety conditions, and parcel characteristics such as size and weight.

Figure 8 confirms that both the total reservation count and the surrogate objective value decrease as $\overline{d}$ increases. This reduction exhibits a convex pattern and converges to a lower bound. This bound corresponds to the relaxed case $\overline{d} \to \infty$, where logistic vehicle drivers are assumed to park at any location regardless of proximity to the commercial establishments. Under this relaxation, the total reservation count in the baseline test case drops to zero, and the surrogate objective value converges to 3.852. Importantly, around the baseline value of $\overline{d} = 40$ meters, the reservation count shows limited sensitivity to marginal changes in the walking threshold, suggesting that our results remain robust to moderate deviations from the baseline assumption.

Insight 5. *Consideration of walking distance and its threshold is a critical lever in the management of SOPP for logistic vehicles. Although relaxing the walking distance threshold leads to structurally different (and operationally unrealistic) solutions, the system performance remains robust for practically acceptable thresholds in the range of 30–50 meters, without requiring extreme assumptions on drivers' willingness to walk.*

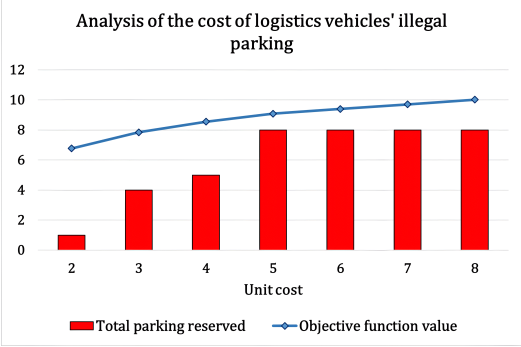

Figure 7: Effect of varying cost of logistic vehicles' blocked parking on the surrogate objective function value and total parking reservation

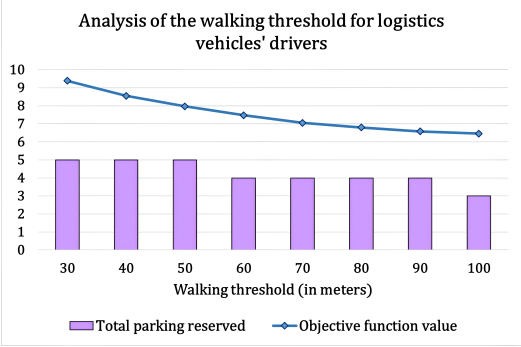

Figure 8: Effect of varying walking distance thresholds on the surrogate objective function value and total parking reservation

6.3 Bidirectional Street Analysis

In this section, we examine an extended scenario in which logistic vehicle drivers can park on the opposite curb of a dual carriageway while serving a delivery location on the current side of the street. To approximate this setting, we extend the original test case to a bidirectional configuration by duplicating the studied street segment on the opposite side. This modeling choice is supported by the structural symmetry between the two sides of SMY Street and by the case study of Darendeliler et al. (2026), which considers both directions of the street. Accordingly, the original index sets $\mathcal{I} = \{1, \ldots, 47\}$ and $\mathcal{J} = \{1, \ldots, 35\}$ are expanded to $\mathcal{I}' = \{1, \ldots, 94\}$ and $\mathcal{J}' = \{1, \ldots, 70\}$. To preserve overall traffic intensity, passenger vehicle arrival rates λ_2 from Scenario 1 are doubled, while $\lambda_{1j} = \lambda_{1(|\mathcal{J}|+j)}$ $\forall j \in \mathcal{J}$ and all departure rates remain unchanged.

Walking distances are adjusted to account for cross-street movements. If a commercial establishment and a parking space are located on the same side of the street, we retain the original distances from the test case for both sides. Otherwise, we assume a Manhattan-type walking path: the driver first crosses the street and then proceeds longitudinally towards the establishment. This is implemented by adding a rough estimate of 10 meters to the corresponding entries in the original distance matrix, representing the direct distance between two facing parking spots across the street. Based on the updated distance matrix, the feasible parking sets δ_j are recomputed using the 40-meter walking distance threshold. All other model parameters remain unchanged. We further assume that passenger vehicles are parked uniformly on both sides of the street.

A comparative analysis of the single-sided and dual-sided configurations is reported in Table 7. We observe that cross-street optimization of parking reservations can improve the surrogate objective value by $100 \times \frac{13.579-12.320}{13.579} = 9.27\%$. The value 13.579 is obtained by evaluating the decomposed-and-merged solution within the surrogate objective function of the joint optimization model. This ensures that the reported performance reflects the actual cost of cross-street interactions, rather than simply doubling the objective value from single-side optimization. Figure 9 illustrates the reservation pattern under the joint optimization model. Unlike the decomposed-and-merged model, the joint model explicitly captures (i) the effective increase in usable parking capacity for logistic vehicles and (ii) the spatial interaction between facing parking spaces across the street. In particular, it accounts for the overlap and substitution effects between opposite-side reservations, which are ignored when each side is optimized in isolation.

Insight 6. *Flexibility in cross-street parking has operational value. Situations where logistic vehicle drivers can utilize parking spaces on both sides of a street effectively enlarge the feasible parking capacity without physically increasing infrastructure. Ignoring this interaction leads to nearly a 9% performance loss. Our framework can accommodate both restricted same-side parking and flexible cross-street parking. An implicit finding of this analysis is that street length does not significantly influence the reservation count. When the street length was doubled, the number of reservations on each side remained unchanged compared to the original test case. This indicates that reservations are primarily driven by demand–supply interactions and spatial constraints, rather than by the physical length of the street itself.*

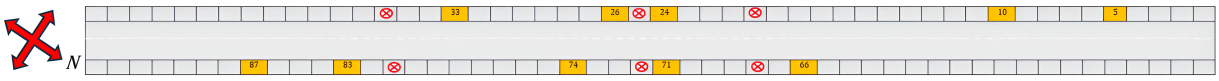

Figure 9: Spatial representation of the parking spaces reserved (highlighted spaces), considering cross-street parking for logistic vehicles. No parking spaces are available in the circled X spots.

Table 7: Performance comparison of parking reservation under cross-street parking flexibility. The decomposed approach optimizes each side independently and then merges the solutions, whereas the joint approach simultaneously optimizes both sides while accounting for spatial interactions between facing parking spaces.

Approach	Selected street indices	Total reservations	Surrogate objective value
Single-side optimization	[7, 18, 24, 27, 37]	5	8.555
Both sides (decomposed and merged)	[7, 18, 24, 27, 37, 42, 53, 59, 62, 72]	10	13.579
Both sides (joint optimization)	[5, 10, 24, 26, 33, 66, 71, 74, 83, 87]	10	12.320

7 Conclusion

In this study, we propose a location-aware on-street parking space reservation SOPP framework for logistic vehicles in a bi-modal urban parking system. Unlike existing aggregate models, which determine only the total number of logistic bays, our framework explicitly accounts for the spatial distribution of parking spaces, walking-distance constraints, and the interdependence between logistic and passenger demand. In SOPP, passenger vehicles may park freely in any unreserved space, while logistic vehicles park within a walking-distance threshold of their delivery destinations. We formulate the SOPP as a bilevel optimization model in which the upper level determines parking space reservations, while the lower level embeds a CTMC to evaluate location-dependent blocking probabilities and the resulting societal costs arising from increased traffic delays and emissions. The objective is to minimize the costs associated with parking blockages, which lead to illegal parking by logistic vehicles and cruising by passenger vehicles. To address the resulting computational challenges, we develop a tractable surrogate model based on a quadratic Boolean approximation.

Our findings reveal that parking provision for logistic vehicles is inherently interdependent and cannot be determined by a simple threshold-based approach or add-drop heuristic. In particular, reserving one space alters the effective distribution of passenger and logistic demand, which in turn affects blocking probabilities and adequate service levels at neighboring spaces. That said, suboptimal parking provision can create underutilized spaces that fail to support last-mile operations effectively and, even counterintuitively, can increase illegal parking by logistic vehicles elsewhere along the street. We found that a location-ignorant approach yields suboptimal, inefficient solutions for SOPP. In our test case, such a policy suggested zero reservations and exhibited a performance gap of approximately 15% relative to our proposed method. Under traffic-intensive conditions, this gap exceeded 30%, revealing that such ignorance becomes increasingly misleading as congestion intensifies. Our results also indicated that both the number of reservations and the overall cost vary linearly with the ratio of passenger-to-logistic arrival rates. In contrast, these performance indicators display diminishing marginal effects with respect to the departure rate ratio of logistic vehicles to passenger vehicles, the cost coefficient ratio, i.e., the relative cost of a logistic vehicle blockage compared to a passenger vehicle blockage, and the walking distance threshold. Thus, we rank the parameters in descending order of influence as follows: (i) the ratio of arrival rates, (ii) the walking distance threshold, (iii) the cost coefficient ratio, and (iv) the ratio of departure rates.

We used an estimate of the peak time asymptotic arrival rate of logistic and passenger vehicles to the street in our test case and designed scenarios with establishment-specific arrival rates. Accurately computing delivery demand for each establishment or accounting for time-varying arrivals remains a key limitation. Future research could address this challenge through empirical surveys to more precisely capture establishment-specific or time-dependent arrival rates across the study region. Nevertheless, as shown in Table 4, we observed no significant change in the reservation count or incurred costs across scenarios, suggesting the robustness of the asymptotic assumption. The proposed framework can also be extended to multi-street networks where applicable. In addition, temporal reservation systems may be investigated alongside permanent on-street parking reservations to back up irregular peaks in arrival rates.

Acknowledgements

This research was supported by ERC Starting Grant 101076231.

Declaration

The authors declare no potential conflicts of interest with respect to the research, authorship, and/or publication of this article.

Data availability

Code and data files will be shared on request.

References

Abdeen, M. A., Nemer, I. A., & Sheltami, T. R. (2021). A balanced algorithm for in-city parking allocation: A case study of Al Madinah City. *Sensors*, *21*, 3148.

Abhishek, Legros, B., & Fransoo, J. C. (2021). Performance evaluation of stochastic systems with dedicated delivery bays and general on-street parking. *Transportation Science*, *55*, 1070–1087.

Amer, A., & Chow, J. Y. (2017). A downtown on-street parking model with urban truck delivery behavior. *Transportation Research Part A: Policy and Practice*, *102*, 51–67.

Burns, A., Forsythe, C. R., Michalek, J. J., & Whitefoot, K. (2025). Estimating the potential for dynamic parking reservation systems to increase delivery vehicle accommodation. *Transportation Research Part A: Policy and Practice*, *193*, 104380.

Caliskan, M., Barthels, A., Scheuermann, B., & Mauve, M. (2007). Predicting parking lot occupancy in vehicular ad hoc networks. In *2007 IEEE 65th Vehicular Technology Conference-VTC2007-Spring* (pp. 277–281). IEEE.

Campbell, S., Holguín-Veras, J., Ramirez-Rios, D. G., González-Calderón, C., Kalahasthi, L., & Wojtowicz, J. (2018). Freight and service parking needs and the role of demand management. *European Transport Research Review*, *10*, 47.

Castrellon, J. P., & Sanchez-Diaz, I. (2024). Effects of freight curbside management on sustainable cities: Evidence and paths forward. *Transportation Research Part D: Transport and Environment*, *130*, 104165.

Chiara, G. D., Cheah, L., Azevedo, C. L., & Ben-Akiva, M. E. (2020). A policy-sensitive model of parking choice for commercial vehicles in urban areas. *Transportation Science*, *54*, 606–630.

Dalla Chiara, G., & Cheah, L. (2017). Data stories from urban loading bays. *European Transport Research Review*, *9*, 50.

Dalla Chiara, G., Krutein, K. F., Ranjbari, A., & Goodchild, A. (2021). Understanding urban commercial vehicle driver behaviors and decision making. *Transportation Research Record*, *2675*, 608–619.

Darendeliler, A., Yıldız, B., & Karaesmen, F. (2026). Dynamic and robust allocation of on-street parking for passenger and delivery vehicles. *Optimization Online*, (p. 33776). URL: https://optimization-online.org/?p=33736.

Dowling, C. P., Ratliff, L. J., & Zhang, B. (2019). Modeling curbside parking as a network of finite capacity queues. *IEEE Transactions on Intelligent Transportation Systems*, *21*, 1011–1022.

Dutta, N., Charlottin, T., & Nicolas, A. (2023). Parking search in the physical world: Calculating the search time by leveraging physical and graph theoretical methods. *Transportation Science*, *57*, 685–700.

Eurostat (2026). Passenger cars in the EU. https://ec.europa.eu/eurostat/statistics-explained/index.php?title=Passenger_cars_in_the_EU, last accessed 02.25.2026.

Fransoo, J. C., Cedillo-Campos, M. G., & Gamez-Perez, K. M. (2022). Estimating the benefits of dedicated unloading bays by field experimentation. *Transportation Research Part A: Policy and Practice*, *160*, 348–354.

Fulman, N., & Benenson, I. (2021). Approximation method for estimating search times for on-street parking. *Transportation Science*, *55*, 1046–1069.

Ghizzawi, F., Galal, A., & Roorda, M. J. (2024). Modelling parking behaviour of commercial vehicles: a scoping review. *Transport Reviews*, *44*, 743–765.

Goodchild, A., & Ivanov, B. (2017). The final 50 feet of the urban goods delivery system. *System*, *54*, 55.

Hampshire, R. C., & Shoup, D. (2018). What share of traffic is cruising for parking? *Journal of Transport Economics and Policy (JTEP)*, *52*, 184–201.

Han, L. D., Chin, S.-M., Franzese, O., & Hwang, H. (2005). Estimating the impact of pickup-and delivery-related illegal parking activities on traffic. *Transportation Research Record*, *1906*, 49–55.

Ismael, A., & Holguin-Veras, J. (2025). Optimal parking allocation for heterogeneous vehicle types. *Transportation Research Part A: Policy and Practice*, *192*, 104357.

Kim, W., & Wang, X. (2022). Double parking in new york city: a comparison between commercial vehicles and passenger vehicles. *Transportation*, *49*, 1315–1337.

Kin, B., Verlinde, S., & Macharis, C. (2017). Sustainable urban freight transport in megacities in emerging markets. *Sustainable Cities and Society*, *32*, 31–41.

Legros, B., & Fransoo, J. C. (2024). Admission and pricing optimization of on-street parking with delivery bays. *European Journal of Operational Research*, *312*, 138–149.

Liu, J., & Qian, S. (2024). Modeling multimodal curbside usage in dynamic networks. *Transportation Science*, *58*, 1277–1299.

Liu, X., Qian, S., Teo, H.-H., & Ma, W. (2024). Estimating and mitigating the congestion effect of curbside pick-ups and drop-offs: A causal inference approach. *Transportation Science*, *58*, 355–376.

Liu, Y., Pan, S., Folz, P., Ramparany, F., Bolle, S., Ballot, E., & Coupaye, T. (2023). Cognitive digital twins for freight parking management in last mile delivery under smart cities paradigm. *Computers in Industry*, *153*, 104022.

Mora-Quiñones, C. A., Fransoo, J. C., Velázquez-Martínez, J. C., Cárdenas-Barrón, L. E., & Escamilla, R. (2024). Assessing the impact of loading-unloading zones in emerging markets: Evidence from Mexico. *Transportation Research Part D: Transport and Environment*, *137*, 104486.

Nourinejad, M., Wenneman, A., Habib, K. N., & Roorda, M. J. (2014). Truck parking in urban areas: Application of choice modelling within traffic microsimulation. *Transportation Research Part A: Policy and Practice*, *64*, 54–64.

Reed, S., Campbell, A. M., & Thomas, B. W. (2024). Does parking matter? The impact of parking time on last-mile delivery optimization. *Transportation Research Part E: Logistics and Transportation Review*, *181*, 103391.

Ross, S. M. (2014). *Introduction to probability models*. Academic press.

Schmid, J., Wang, X. C., & Conway, A. (2018). Commercial vehicle parking duration in new york city and its implications for planning. *Transportation Research Part A: Policy and Practice*, *116*, 580–590.

e Silva, J. d. A., & Alho, A. R. (2017). Using structural equations modeling to explore perceived urban freight deliveries parking issues. *Transportation Research Part A: Policy and Practice*, *102*, 18–32.

Silva, K., da Silva Lima, R., Alves, R., Yushimito, W. F., & Holguín-Veras, J. (2020). Freight and service parking needs in historical centers: a case study in são joão del rei, brazil. *Transportation Research Record*, *2674*, 352–366.

Vieira, J. G. V., & Fransoo, J. C. (2015). How logistics performance of freight operators is affected by urban freight distribution issues. *Transport Policy*, *44*, 37–47.

World Economic Forum (2020). The Future of the Last-Mile Ecosystem. https://www.weforum.org/publications/the-future-of-the-last-mile-ecosystem/, last accessed 02.25.2026.

Xiao, J., Lou, Y., & Frisby, J. (2018). How likely am i to find parking?A practical model-based framework for predicting parking availability. *Transportation Research Part B: Methodological*, *112*, 19–39.

E-Companion to: Optimizing Spatial On-street Parking Provision for Logistic Vehicles

Amirreza Pashapour *, Barış Yıldız †

EC.1 Proofs

Proof of Proposition 3.1.

Proof. We give a polynomial-time reduction from the $\mathcal{NP}$-complete Subset-Sum problem. Let an instance of Subset-Sum be given by an array of n positive integers $\{a_1, \ldots, a_n\}$ and target sum T. We construct a bilevel instance as follows.

Upper level: choose a binary vector $\mathbf{x} \in \{0,1\}^n$.

Lower level: define a CTMC with state space $S = \{0, 1, \ldots, n\}$ of size $n+1$. For each state $s \in \{1, \ldots, n\}$ set the transition rate from state 0 to state i equal to $x_i a_i$, and the rate from state i to state 0 equal to 1. (All other transition rates are 0.) Let $Q(\mathbf{x})$ be the generator matrix of this CTMC and let $\pi(\mathbf{x})$ denote its steady-state distribution, i.e., the unique solution of

$$\pi(\mathbf{x})^\top Q(\mathbf{x}) = 0, \qquad \sum_{s=0}^{n} \pi_s(\mathbf{x}) = 1.$$

For this CTMC the steady-state equations for $s = 1, \ldots, n$ let

$$\pi_i(\mathbf{x}) = \pi_0(\mathbf{x})\, x_i a_i \quad (i = 1, \ldots, n).$$

Using the normalization constraint,

$$\pi_0(\mathbf{x}) + \sum_{i=1}^{n} \pi_i(\mathbf{x}) = \pi_0(\mathbf{x})\Big(1 + \sum_{i=1}^{n} x_i a_i\Big) = 1,$$

so

$$\pi_0(\mathbf{x}) = \frac{1}{1 + S(\mathbf{x})}, \qquad S(\mathbf{x}) := \sum_{i=1}^{n} x_i a_i.$$

*School of Management, University of Bath, Bath BA2 7AY, United Kingdom; Email: ap3903@bath.ac.uk
†Department of Industrial Engineering, Koç University, Istanbul 34450, Türkiye; Email: byildiz@ku.edu.tr

Thus the lower-level solution $\pi(\mathbf{x})$ can be computed in polynomial time given $\mathbf{x}$, and in particular the scalar $S(\mathbf{x})$ (the sum of selected a_i) is recovered from $\pi_0(\mathbf{x})$ via $S(\mathbf{x}) = \frac{1}{\pi_0(\mathbf{x})} - 1$ for a given binary $\mathbf{x}$ vector. Now define the upper-level objective to be whether there exists $\mathbf{x} \in \{0,1\}^n$ such that

$$C(\mathbf{x}, \pi(\mathbf{x})) := |S(\mathbf{x}) - T| = \left| \frac{1}{\pi_0(\mathbf{x})} - 1 - T \right| = 0.$$

This equality holds if and only if $S(\mathbf{x}) = T$, i.e. iff there exists a subset of the a_i's summing to T. Therefore, the SUBSET-SUM instance has a solution iff the constructed bilevel decision instance above has a feasible $\mathbf{x}$ with objective value 0. The reduction is polynomial-time, so the SOPP bilevel decision problem is $\mathcal{NP}$-hard. □

EC.2 An Illustrative Example

Consider a synthetically short street with $\mathcal{I} = \{1, \ldots, 8\}$ parking spaces and $\mathcal{J} = \{1, \ldots, 4\}$ delivery addresses, as depicted in Figure EC.1. The distance matrix between parking spaces and addresses is provided in Table EC.1, and we set the distance threshold to $\overline{d} = 10$ meters. The arrival rates for logistic vehicles are $\lambda_{1j} = \{1:2, 2:1.5, 3:1, 4:0.5\}$ per hour, while passenger vehicles arrive at a rate $\lambda_2 = 15$ per hour. Service rates are set to $\mu_1 = 3$ and $\mu_2 = 2$ vehicles per hour for logistic and passenger vehicles, respectively. We further set cost parameters to $\alpha_1 = 3$ and $\alpha_2 = 2$.

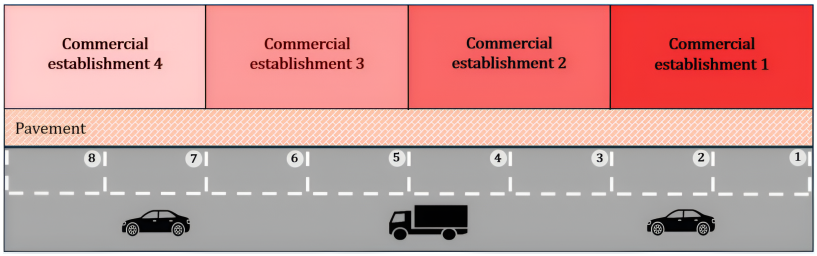

Figure EC.1: Schematic Street layout for the illustrative example.

Table EC.1: A Synthetic Distance matrix (in meters)

		$j \in \mathcal{J}$			
		1	2	3	4
$i \in \mathcal{I}$	1	5	15	25	35
	2	5	10	20	30
	3	10	5	15	25
	4	15	5	10	20
	5	20	10	5	15
	6	25	15	5	10
	7	30	20	10	5
	8	35	25	15	5

This instance yields $2^8 = 256$ distinct reservation vectors. Given this manageable size, we enumerate and evaluate all $\mathbf{x}$ vectors exactly. Solving the full model for each $\mathbf{x}$, we report the results in Tables EC.3

and EC.4. These tables represent solution ID ranging from 1 to 256, the solution vector, the expected total blocked events as Ω_1 and Ω_2 for logistic and passenger vehicles, respectively, the total cost $C(\mathbf{x})$ from the bi-level model, and the surrogate function value $g(\mathbf{x})$. The optimal reservation vectors, which yield the minimum $C(\mathbf{x})$ value, are $\mathbf{x}^* = \{0, 1, 0, 0, 0, 0, 0, 0\}$ and $\mathbf{x}^* = \{0, 0, 1, 0, 0, 0, 0, 0\}$, each achieving a total cost of 15.295 units (highlighted as IDs 33 and 65 in Table EC.3).

The process of initializing and obtaining the $g(\mathbf{x})$ values is described next.

1. **Data farming.** We enrich the DES dataset by generating $N = 250$ samples, each evaluated with $r = 500$ replications over a planning horizon of $H = 8$. The reservation density is set to $m = 0.1$, and the resulting dataset is split into 80/20% train and test partitions.

2. **Surrogate model estimation.** Using the sampled observations, we fit a quadratic regression model to obtain a surrogate function $g(\mathbf{x})$. The resulting R^2 for the test set is reported as 0.96. The estimated coefficients are reported in Table EC.2, where diagonal entries correspond to linear terms and off-diagonal entries correspond to quadratic interaction terms $x_i x_j$, with intercept reported as 15.7729.

3. **Surrogate optimization.** We then solve the surrogate function $g(\mathbf{x})$, which yields the surrogate-optimal solution, $\mathbf{x}^* = \{0, 0, 1, 0, 0, 0, 0, 0\}$, with an estimated cost of $g(\mathbf{x}^*) = 15.725$ (ID 33) and with an estimation gap of $100 \times (15.725 - 15.295)/15.295 = 2.81\%$ with respect to the optimal solution of the bi-level model. In this instance, optimizing the surrogate objective function accurately returned the true optimal reservation decision.

The exhaustive solution of the bi-level model over the full set of reservation vectors required roughly 12 minutes. The associated computational complexity increases sharply with the number of parking spaces, and becomes impractical for street sizes of $|\mathcal{I}| \geq 10$. In comparison, the proposed methodology, which integrates data farming, surrogate modeling, and surrogate optimization, completed this instance in less than 30 seconds.

We illustrate the $C(\mathbf{x})$ and $g(\mathbf{x})$ values in Figure EC.2. In this figure, solutions are ordered non-decreasingly according to the bi-level model results $C(\mathbf{x})$. The average absolute gap between $C(\mathbf{x})$ and $g(\mathbf{x})$ across all 256 reservation vectors is obtained as 0.56% .

As a final remark regarding Theorem 1, we demonstrate the non-monotonicity of Ω_1 with respect to $\mathbf{1}^\top \mathbf{x}$ using a counterexample. Consider the following reservation vectors from Table EC.3:

- ID 9: {0,0,0,0,1,0,0,0},
- ID 13: {0,0,0,0,1,1,0,0},
- ID 15: {0,0,0,0,1,1,1,0},
- ID 16: {0,0,0,0,1,1,1,1}.

As the number of reserved spaces increases along this sequence, the value of Ω_1 decreases from 2.016 (ID 9) to 1.727 (ID 13) and then to 1.657 (ID 15), but subsequently increases to 1.704 (ID 16). This confirms that

Ω_1 is not monotone in the reservation count. By contrast, Ω_2 exhibits the monotonic increase considering this example and across all the vectors with respect to $\mathbf{1}^\top \mathbf{x}$.

Table EC.2: Matrix of Interaction Coefficients of the Surrogate Function $g(\mathbf{x})$ (Intercept = 15.7729)

	x_1	x_2	x_3	x_4	x_5	x_6	x_7	x_8
x_1	0.5754	0.4360	0.5048	–	–	–	–	–
x_2	–	0.0354	0.6571	0.4603	0.2953	–	–	–
x_3	–	–	-0.0483	0.2602	0.3056	–	–	–
x_4	–	–	–	0.4027	0.0000	0.2352	0.4104	–
x_5	–	–	–	–	0.4218	0.4477	0.3665	–
x_6	–	–	–	–	–	1.0294	0.8527	0.4049
x_7	–	–	–	–	–	–	0.9956	0.5695
x_8	–	–	–	–	–	–	–	1.9500

Table EC.3: Optimal results for all reservation vectors (part I) (* Best: IDs 33 and 65)

ID	x_1	x_2	x_3	x_4	x_5	x_6	x_7	x_8	Ω_1	Ω_2	$C(\mathbf{x})$	$g(\mathbf{x})$
1	0	0	0	0	0	0	0	0	2.517	3.967	15.485	15.773
2	0	0	0	0	0	0	0	1	2.455	5.060	17.485	17.723
3	0	0	0	0	0	0	1	0	2.177	4.972	16.475	16.769
4	0	0	0	0	0	0	1	1	2.202	6.211	19.028	19.288
5	0	0	0	0	0	1	0	0	2.177	4.972	16.475	16.802
6	0	0	0	0	0	1	0	1	2.202	6.211	19.028	19.157
7	0	0	0	0	0	1	1	0	2.095	6.155	18.595	18.651
8	0	0	0	0	0	1	1	1	2.172	7.523	21.562	21.575
9	0	0	0	0	1	0	0	0	2.016	4.902	15.852	16.195
10	0	0	0	0	1	0	0	1	1.884	6.116	17.884	18.145
11	0	0	0	0	1	0	1	0	1.727	6.054	17.289	17.557
12	0	0	0	0	1	0	1	1	1.721	7.408	19.979	20.076
13	0	0	0	0	1	1	0	0	1.727	6.054	17.289	17.672
14	0	0	0	0	1	1	0	1	1.721	7.408	19.979	20.027
15	0	0	0	0	1	1	1	0	1.657	7.368	19.707	19.887
16	0	0	0	0	1	1	1	1	1.704	8.837	22.786	22.811
17	0	0	0	1	0	0	0	0	2.016	4.902	15.852	16.176
18	0	0	0	1	0	0	0	1	1.884	6.116	17.884	18.126
19	0	0	0	1	0	0	1	0	1.727	6.054	17.289	17.582
20	0	0	0	1	0	0	1	1	1.721	7.408	19.979	20.101
21	0	0	0	1	0	1	0	0	1.727	6.054	17.289	17.440
22	0	0	0	1	0	1	0	1	1.721	7.408	19.979	19.795
23	0	0	0	1	0	1	1	0	1.657	7.368	19.707	19.699
24	0	0	0	1	0	1	1	1	1.704	8.837	22.786	22.623
25	0	0	0	1	1	0	0	0	1.744	6.019	17.270	16.597
26	0	0	0	1	1	0	0	1	1.568	7.348	19.400	18.547
27	0	0	0	1	1	0	1	0	1.507	7.309	19.139	18.370
28	0	0	0	1	1	0	1	1	1.491	8.765	22.003	20.889
29	0	0	0	1	1	1	0	0	1.507	7.309	19.139	18.310
30	0	0	0	1	1	1	0	1	1.491	8.765	22.003	20.664
31	0	0	0	1	1	1	1	0	1.464	8.740	21.872	20.935
32	0	0	0	1	1	1	1	1	1.500	10.297	25.094	23.859
33*	**0**	**0**	1	**0**	**0**	**0**	**0**	**0**	**1.863**	**4.853**	**15.295**	**15.725**
34	0	0	1	0	0	0	0	1	1.724	6.065	17.302	17.675
35	0	0	1	0	0	0	1	0	1.435	5.973	16.251	16.720
36	0	0	1	0	0	0	1	1	1.394	7.322	18.826	19.240
37	0	0	1	0	0	1	0	0	1.435	5.973	16.251	16.754
38	0	0	1	0	0	1	0	1	1.394	7.322	18.826	19.109
39	0	0	1	0	0	1	1	0	1.285	7.265	18.385	18.602
40	0	0	1	0	0	1	1	1	1.303	8.732	21.373	21.527
41	0	0	1	0	1	0	0	0	1.378	5.931	15.996	16.452
42	0	0	1	0	1	0	0	1	1.181	7.257	18.057	18.402
43	0	0	1	0	1	0	1	0	1.040	7.196	17.512	17.814
44	0	0	1	0	1	0	1	1	0.985	8.651	20.257	20.334
45	0	0	1	0	1	1	0	0	1.040	7.196	17.512	17.929
46	0	0	1	0	1	1	0	1	0.985	8.651	20.257	20.284
47	0	0	1	0	1	1	1	0	0.931	8.613	20.019	20.144
48	0	0	1	0	1	1	1	1	0.936	10.171	23.150	23.068
49	0	0	1	1	0	0	0	0	1.378	5.931	15.996	16.387
50	0	0	1	1	0	0	0	1	1.181	7.257	18.057	18.337
51	0	0	1	1	0	0	1	0	1.040	7.196	17.512	17.794
52	0	0	1	1	0	0	1	1	0.985	8.651	20.257	20.313
53	0	0	1	1	0	1	0	0	1.040	7.196	17.512	17.652
54	0	0	1	1	0	1	0	1	0.985	8.651	20.257	20.007
55	0	0	1	1	0	1	1	0	0.931	8.613	20.019	19.911
56	0	0	1	1	0	1	1	1	0.936	10.171	23.150	22.835
57	0	0	1	1	1	0	0	0	1.118	7.183	17.720	17.115
58	0	0	1	1	1	0	0	1	0.888	8.614	19.892	19.065
59	0	0	1	1	1	0	1	0	0.843	8.576	19.681	18.887
60	0	0	1	1	1	0	1	1	0.789	10.123	22.613	21.407
61	0	0	1	1	1	1	0	0	0.843	8.576	19.681	18.827
62	0	0	1	1	1	1	0	1	0.789	10.123	22.613	21.182
63	0	0	1	1	1	1	1	0	0.769	10.099	22.505	21.452
64	0	0	1	1	1	1	1	1	0.771	11.733	25.779	24.377
65*	**0**	**1**	**0**	**0**	**0**	**0**	**0**	**0**	**1.863**	**4.853**	**15.295**	**15.808**
66	0	1	0	0	0	0	0	1	1.724	6.065	17.302	17.758
67	0	1	0	0	0	0	1	0	1.435	5.973	16.251	16.804
68	0	1	0	0	0	0	1	1	1.394	7.322	18.826	19.323
69	0	1	0	0	0	1	0	0	1.435	5.973	16.251	16.838
70	0	1	0	0	0	1	0	1	1.394	7.322	18.826	19.193
71	0	1	0	0	0	1	1	0	1.285	7.265	18.385	18.686
72	0	1	0	0	0	1	1	1	1.303	8.732	21.373	21.610
73	0	1	0	0	1	0	0	0	1.378	5.931	15.996	16.525
74	0	1	0	0	1	0	0	1	1.181	7.257	18.057	18.475
75	0	1	0	0	1	0	1	0	1.040	7.196	17.512	17.888
76	0	1	0	0	1	0	1	1	0.985	8.651	20.257	20.407
77	0	1	0	0	1	1	0	0	1.040	7.196	17.512	18.002
78	0	1	0	0	1	1	0	1	0.985	8.651	20.257	20.357
79	0	1	0	0	1	1	1	0	0.931	8.613	20.019	20.217
80	0	1	0	0	1	1	1	1	0.936	10.171	23.150	23.142
81	0	1	0	1	0	0	0	0	1.378	5.931	15.996	16.671
82	0	1	0	1	0	0	0	1	1.181	7.257	18.057	18.621
83	0	1	0	1	0	0	1	0	1.040	7.196	17.512	18.077
84	0	1	0	1	0	0	1	1	0.985	8.651	20.257	20.597
85	0	1	0	1	0	1	0	0	1.040	7.196	17.512	17.936
86	0	1	0	1	0	1	0	1	0.985	8.651	20.257	20.291
87	0	1	0	1	0	1	1	0	0.931	8.613	20.019	20.195
88	0	1	0	1	0	1	1	1	0.936	10.171	23.150	23.119
89	0	1	0	1	1	0	0	0	1.118	7.183	17.720	17.388
90	0	1	0	1	1	0	0	1	0.888	8.614	19.892	19.338
91	0	1	0	1	1	0	1	0	0.843	8.576	19.681	19.161
92	0	1	0	1	1	0	1	1	0.789	10.123	22.613	21.680
93	0	1	0	1	1	1	0	0	0.843	8.576	19.681	19.101
94	0	1	0	1	1	1	0	1	0.789	10.123	22.613	21.455
95	0	1	0	1	1	1	1	0	0.769	10.099	22.505	21.726
96	0	1	0	1	1	1	1	1	0.771	11.733	25.779	24.650
97	0	1	1	0	0	0	0	0	1.385	5.918	15.991	16.417
98	0	1	1	0	0	0	0	1	1.194	7.245	18.072	18.367
99	0	1	1	0	0	0	1	0	0.891	7.151	16.975	17.413
100	0	1	1	0	0	0	1	1	0.809	8.603	19.633	19.932
101	0	1	1	0	0	1	0	0	0.891	7.151	16.975	17.446
102	0	1	1	0	0	1	0	1	0.809	8.603	19.633	19.801
103	0	1	1	0	0	1	1	0	0.697	8.545	19.181	19.295
104	0	1	1	0	0	1	1	1	0.681	10.102	22.247	22.219
105	0	1	1	0	1	0	0	0	0.941	7.136	17.095	17.440
106	0	1	1	0	1	0	0	1	0.704	8.567	19.246	19.390
107	0	1	1	0	1	0	1	0	0.578	8.507	18.748	18.802
108	0	1	1	0	1	0	1	1	0.498	10.053	21.600	21.321
109	0	1	1	0	1	1	0	0	0.578	8.507	18.748	18.917
110	0	1	1	0	1	1	0	1	0.498	10.053	21.600	21.272
111	0	1	1	0	1	1	1	0	0.453	10.017	21.393	21.132
112	0	1	1	0	1	1	1	1	0.438	11.652	24.618	24.056
113	0	1	1	1	0	0	0	0	0.941	7.136	17.095	17.540
114	0	1	1	1	0	0	0	1	0.704	8.567	19.246	19.490
115	0	1	1	1	0	0	1	0	0.578	8.507	18.748	18.946
116	0	1	1	1	0	0	1	1	0.498	10.053	21.600	21.466
117	0	1	1	1	0	1	0	0	0.578	8.507	18.748	18.805
118	0	1	1	1	0	1	0	1	0.498	10.053	21.600	21.160
119	0	1	1	1	0	1	1	0	0.453	10.017	21.393	21.064
120	0	1	1	1	0	1	1	1	0.438	11.652	24.618	23.988
121	0	1	1	1	1	0	0	0	0.722	8.513	19.192	18.563
122	0	1	1	1	1	0	0	1	0.459	10.035	21.447	20.513
123	0	1	1	1	1	0	1	0	0.430	10.001	21.292	20.335
124	0	1	1	1	1	0	1	1	0.357	11.625	24.321	22.855
125	0	1	1	1	1	1	0	0	0.430	10.001	21.292	20.275
126	0	1	1	1	1	1	0	1	0.357	11.625	24.321	22.630
127	0	1	1	1	1	1	1	0	0.345	11.603	24.241	22.900
128	0	1	1	1	1	1	1	1	0.333	13.302	27.603	25.825

Table EC.4: Optimal results for all reservation vectors (part II) (* Best: IDs 33 and 65)

ID	x_1	x_2	x_3	x_4	x_5	x_6	x_7	x_8	Ω_1	Ω_2	$C(\mathbf{x})$	$g(\mathbf{x})$
129	1	0	0	0	0	0	0	0	2.017	4.948	15.947	16.348
130	1	0	0	0	0	0	0	1	1.892	6.165	18.006	18.298
131	1	0	0	0	0	0	1	0	1.600	6.073	16.946	17.344
132	1	0	0	0	0	0	1	1	1.573	7.426	19.571	19.863
133	1	0	0	0	0	1	0	0	1.600	6.073	16.946	17.378
134	1	0	0	0	0	1	0	1	1.573	7.426	19.571	19.733
135	1	0	0	0	0	1	1	0	1.462	7.369	19.124	19.226
136	1	0	0	0	0	1	1	1	1.496	8.837	22.162	22.150
137	1	0	0	0	1	0	0	0	1.434	5.999	16.300	16.770
138	1	0	0	0	1	0	0	1	1.243	7.328	18.385	18.720
139	1	0	0	0	1	0	1	0	1.079	7.264	17.765	18.132
140	1	0	0	0	1	0	1	1	1.027	8.719	20.519	20.652
141	1	0	0	0	1	1	0	0	1.079	7.264	17.765	18.247
142	1	0	0	0	1	1	0	1	1.027	8.719	20.519	20.602
143	1	0	0	0	1	1	1	0	0.962	8.680	20.246	20.462
144	1	0	0	0	1	1	1	1	0.970	10.237	23.384	23.386
145	1	0	0	1	0	0	0	0	1.434	5.999	16.300	16.751
146	1	0	0	1	0	0	0	1	1.243	7.328	18.385	18.701
147	1	0	0	1	0	0	1	0	1.079	7.264	17.765	18.157
148	1	0	0	1	0	0	1	1	1.027	8.719	20.519	20.677
149	1	0	0	1	0	1	0	0	1.079	7.264	17.765	18.016
150	1	0	0	1	0	1	0	1	1.027	8.719	20.519	20.370
151	1	0	0	1	0	1	1	0	0.962	8.680	20.246	20.274
152	1	0	0	1	0	1	1	1	0.970	10.237	23.384	23.199
153	1	0	0	1	1	0	0	0	1.100	7.227	17.754	17.173
154	1	0	0	1	1	0	0	1	0.870	8.658	19.926	19.123
155	1	0	0	1	1	0	1	0	0.808	8.619	19.662	18.945
156	1	0	0	1	1	0	1	1	0.751	10.165	22.583	21.465
157	1	0	0	1	1	1	0	0	0.808	8.619	19.662	18.885
158	1	0	0	1	1	1	0	1	0.751	10.165	22.583	21.240
159	1	0	0	1	1	1	1	0	0.724	10.139	22.450	21.510
160	1	0	0	1	1	1	1	1	0.725	11.772	25.719	24.435
161	1	0	1	0	0	0	0	0	1.488	5.994	16.452	16.805
162	1	0	1	0	0	0	0	1	1.305	7.323	18.561	18.755
163	1	0	1	0	0	0	1	0	0.999	7.229	17.455	17.800
164	1	0	1	0	0	0	1	1	0.925	8.682	20.139	20.320
165	1	0	1	0	0	1	0	0	0.999	7.229	17.455	17.834
166	1	0	1	0	0	1	0	1	0.925	8.682	20.139	20.189
167	1	0	1	0	0	1	1	0	0.812	8.625	19.686	19.682
168	1	0	1	0	0	1	1	1	0.804	10.181	22.774	22.607
169	1	0	1	0	1	0	0	0	0.983	7.189	17.327	17.532
170	1	0	1	0	1	0	0	1	0.749	8.621	19.489	19.482
171	1	0	1	0	1	0	1	0	0.606	8.559	18.936	18.894
172	1	0	1	0	1	0	1	1	0.527	10.105	21.791	21.414
173	1	0	1	0	1	1	0	0	0.606	8.559	18.936	19.009
174	1	0	1	0	1	1	0	1	0.527	10.105	21.791	21.364
175	1	0	1	0	1	1	1	0	0.474	10.067	21.556	21.224
176	1	0	1	0	1	1	1	1	0.460	11.701	24.782	24.148
177	1	0	1	1	0	0	0	0	0.983	7.189	17.327	17.468
178	1	0	1	1	0	0	0	1	0.749	8.621	19.489	19.418
179	1	0	1	1	0	0	1	0	0.606	8.559	18.936	18.874
180	1	0	1	1	0	0	1	1	0.527	10.105	21.791	21.393
181	1	0	1	1	0	1	0	0	0.606	8.559	18.936	18.732
182	1	0	1	1	0	1	0	1	0.527	10.105	21.791	21.087
183	1	0	1	1	0	1	1	0	0.474	10.067	21.556	20.991
184	1	0	1	1	0	1	1	1	0.460	11.701	24.782	23.915
185	1	0	1	1	1	0	0	0	0.719	8.549	19.255	18.195
186	1	0	1	1	1	0	0	1	0.457	10.070	21.511	20.145
187	1	0	1	1	1	0	1	0	0.416	10.034	21.316	19.968
188	1	0	1	1	1	0	1	1	0.342	11.657	24.340	22.487
189	1	0	1	1	1	1	0	0	0.416	10.034	21.316	19.907
190	1	0	1	1	1	1	0	1	0.342	11.657	24.340	22.262
191	1	0	1	1	1	1	1	0	0.325	11.634	24.243	22.533
192	1	0	1	1	1	1	1	1	0.312	13.332	27.600	25.457
193	1	1	0	0	0	0	0	0	1.488	5.994	16.452	16.820
194	1	1	0	0	0	0	0	1	1.305	7.323	18.561	18.770
195	1	1	0	0	0	0	1	0	0.999	7.229	17.455	17.815
196	1	1	0	0	0	0	1	1	0.925	8.682	20.139	20.335
197	1	1	0	0	0	1	0	0	0.999	7.229	17.455	17.849
198	1	1	0	0	0	1	0	1	0.925	8.682	20.139	20.204
199	1	1	0	0	0	1	1	0	0.812	8.625	19.686	19.697
200	1	1	0	0	0	1	1	1	0.804	10.181	22.774	22.622
201	1	1	0	0	1	0	0	0	0.983	7.189	17.327	17.537
202	1	1	0	0	1	0	0	1	0.749	8.621	19.489	19.487
203	1	1	0	0	1	0	1	0	0.606	8.559	18.936	18.899
204	1	1	0	0	1	0	1	1	0.527	10.105	21.791	21.418
205	1	1	0	0	1	1	0	0	0.606	8.559	18.936	19.014
206	1	1	0	0	1	1	0	1	0.527	10.105	21.791	21.369
207	1	1	0	0	1	1	1	0	0.474	10.067	21.556	21.229
208	1	1	0	0	1	1	1	1	0.460	11.701	24.782	24.153
209	1	1	0	1	0	0	0	0	0.983	7.189	17.327	17.683
210	1	1	0	1	0	0	0	1	0.749	8.621	19.489	19.633
211	1	1	0	1	0	0	1	0	0.606	8.559	18.936	19.089
212	1	1	0	1	0	0	1	1	0.527	10.105	21.791	21.608
213	1	1	0	1	0	1	0	0	0.606	8.559	18.936	18.947
214	1	1	0	1	0	1	0	1	0.527	10.105	21.791	21.302
215	1	1	0	1	0	1	1	0	0.474	10.067	21.556	21.206
216	1	1	0	1	0	1	1	1	0.460	11.701	24.782	24.130
217	1	1	0	1	1	0	0	0	0.719	8.549	19.255	18.400
218	1	1	0	1	1	0	0	1	0.457	10.070	21.511	20.350
219	1	1	0	1	1	0	1	0	0.416	10.034	21.316	20.172
220	1	1	0	1	1	0	1	1	0.342	11.657	24.340	22.692
221	1	1	0	1	1	1	0	0	0.416	10.034	21.316	20.112
222	1	1	0	1	1	1	0	1	0.342	11.657	24.340	22.467
223	1	1	0	1	1	1	1	0	0.325	11.634	24.243	22.737
224	1	1	0	1	1	1	1	1	0.312	13.332	27.600	25.662
225	1	1	1	0	0	0	0	0	1.164	7.216	17.924	17.933
226	1	1	1	0	0	0	0	1	0.944	8.648	20.128	19.883
227	1	1	1	0	0	0	1	0	0.624	8.552	18.976	18.929
228	1	1	1	0	0	0	1	1	0.524	10.096	21.764	21.448
229	1	1	1	0	0	1	0	0	0.624	8.552	18.976	18.963
230	1	1	1	0	0	1	0	1	0.524	10.096	21.764	21.317
231	1	1	1	0	0	1	1	0	0.406	10.038	21.294	20.811
232	1	1	1	0	0	1	1	1	0.379	11.672	24.481	23.735
233	1	1	1	0	1	0	0	0	0.726	8.543	19.264	18.956
234	1	1	1	0	1	0	0	1	0.467	10.065	21.531	20.906
235	1	1	1	0	1	0	1	0	0.342	10.006	21.038	20.318
236	1	1	1	0	1	0	1	1	0.252	11.629	24.014	22.838
237	1	1	1	0	1	1	0	0	0.342	10.006	21.038	20.433
238	1	1	1	0	1	1	0	1	0.252	11.629	24.014	22.788
239	1	1	1	0	1	1	1	0	0.209	11.594	23.815	22.648
240	1	1	1	0	1	1	1	1	0.187	13.293	27.147	25.572
241	1	1	1	1	0	0	0	0	0.726	8.543	19.264	19.056
242	1	1	1	1	0	0	0	1	0.467	10.065	21.531	21.006
243	1	1	1	1	0	0	1	0	0.342	10.006	21.038	20.462
244	1	1	1	1	0	0	1	1	0.252	11.629	24.014	22.982
245	1	1	1	1	0	1	0	0	0.342	10.006	21.038	20.321
246	1	1	1	1	0	1	0	1	0.252	11.629	24.014	22.676
247	1	1	1	1	0	1	1	0	0.209	11.594	23.815	22.580
248	1	1	1	1	0	1	1	1	0.187	13.293	27.147	25.504
249	1	1	1	1	1	0	0	0	0.524	10.016	21.604	20.079
250	1	1	1	1	1	0	0	1	0.243	11.615	23.959	22.029
251	1	1	1	1	1	0	1	0	0.219	11.582	23.821	21.852
252	1	1	1	1	1	0	1	1	0.139	13.270	26.957	24.371
253	1	1	1	1	1	1	0	0	0.219	11.582	23.821	21.791
254	1	1	1	1	1	1	0	1	0.139	13.270	26.957	24.146
255	1	1	1	1	1	1	1	0	0.129	13.249	26.885	24.417
256	1	1	1	1	1	1	1	1	0.113	15.000	30.339	27.341

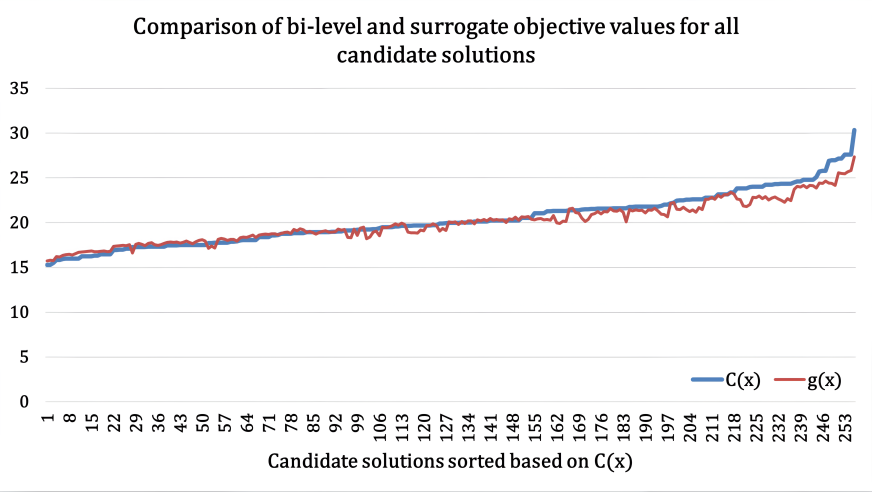

Figure EC.2: Comparison of the objective function values obtained by the bi-level model and the surrogate function across all candidate reservation vectors of the illustrative instance.

Table EC.5: Distance matrix of the test case instances

$\mathcal{I}$ \ $\mathcal{J}$	1	2	3	4	5	6	7	8	9	10	11	12	13	14	15	16	17	18	19	20	21	22	23	24	25	26	27	28	29	30	31	32	33	34	35
1	6	18	25	34	42	54	67	78	88	97	113	136	144	152	165	183	191	200	210	217	225	233	243	252	263	273	283	297	306	314	322	332	345	357	368
2	3	12	19	28	36	48	60	72	82	90	106	130	137	145	159	177	184	194	203	211	219	226	236	245	257	266	276	290	300	308	315	325	339	351	361
3	9	7	13	21	29	41	54	65	75	84	99	123	131	139	152	170	177	187	197	204	212	219	230	238	250	260	270	284	293	301	308	318	332	344	355
4	15	7	8	15	23	34	47	59	68	77	93	116	124	132	146	163	171	181	190	198	205	213	223	232	243	253	263	277	286	295	302	312	325	338	348
5	21	11	6	9	16	28	41	52	62	71	86	110	117	125	139	157	164	174	183	191	199	206	216	225	237	246	257	271	280	288	295	305	319	331	341
6	28	17	10	6	10	22	34	46	55	64	80	103	111	119	132	150	158	167	177	185	192	200	210	219	230	240	250	264	273	281	289	299	312	324	335
7	34	23	15	8	6	15	28	39	49	58	73	97	104	112	126	144	151	161	170	178	186	193	203	212	224	233	243	257	267	275	282	292	306	318	328
8	41	30	22	13	7	9	21	32	42	51	67	90	98	106	119	137	144	154	164	171	179	186	197	205	217	227	237	251	260	268	275	285	299	311	322
9	48	36	28	19	12	5	15	26	36	44	60	83	91	99	113	130	138	148	157	165	173	180	190	199	210	220	230	244	253	262	269	279	292	305	315
10	54	43	34	26	18	7	9	19	29	38	53	77	84	92	106	124	131	141	150	158	166	173	183	192	204	213	224	238	247	255	262	272	286	298	308
11	61	49	41	32	24	13	5	13	23	32	47	70	78	86	100	117	125	134	144	152	159	167	177	186	197	207	217	231	240	248	256	266	279	291	302
12	67	56	47	39	31	19	7	7	16	25	40	64	71	79	93	111	118	128	137	145	153	160	170	179	191	200	210	224	234	242	249	259	272	285	295
13	74	62	54	45	37	25	13	4	10	19	34	57	65	73	86	104	112	121	131	138	146	154	164	172	184	194	204	218	227	235	242	252	266	278	289
14	81	69	61	52	44	32	19	8	5	13	27	51	58	66	80	98	105	115	124	132	140	147	157	166	177	187	197	211	220	229	236	246	259	272	282
15	87	75	67	58	50	38	25	14	6	8	21	44	52	60	73	91	98	108	118	125	133	140	150	159	171	180	191	205	214	222	229	239	253	265	275
16	94	82	74	65	57	45	32	20	11	7	15	38	45	53	67	84	92	102	111	119	126	134	144	153	164	174	184	198	207	215	223	233	246	258	269
17	100	89	80	71	63	51	38	27	17	11	10	31	39	47	60	78	85	95	104	112	120	127	137	146	158	167	177	191	201	209	216	226	239	252	262
18	107	95	87	78	70	58	45	33	24	16	7	25	32	40	54	71	79	88	98	106	113	121	131	140	151	161	171	185	194	202	209	219	233	245	256
19	114	102	94	84	76	64	51	40	30	22	9	18	26	34	47	65	72	82	91	99	107	114	124	133	144	154	164	178	187	195	203	213	226	239	249
20	120	108	100	91	83	71	58	46	37	29	14	12	19	27	41	58	66	75	85	92	100	107	118	126	138	147	158	172	181	189	196	206	220	232	242
21	128	116	108	99	91	79	66	54	44	36	21	6	12	20	33	50	58	68	77	85	92	100	110	119	130	140	150	164	173	181	189	198	212	224	235
22	139	127	119	110	102	90	77	65	56	47	32	9	5	10	22	39	47	56	66	73	81	88	98	107	119	128	139	153	162	170	177	187	201	213	223
23	151	139	130	121	113	101	88	77	67	58	43	19	12	7	11	28	35	45	54	62	70	77	87	96	107	117	127	141	150	158	166	176	189	202	212
24	162	150	142	133	125	112	99	88	78	70	54	30	23	16	5	17	24	34	43	51	59	66	76	85	96	106	116	130	139	147	155	165	178	190	201
25	223	211	202	193	185	173	160	149	139	130	115	91	83	75	62	44	37	27	18	11	6	7	15	24	35	45	55	69	78	86	94	104	117	129	140
26	229	217	209	200	192	180	167	155	145	137	121	97	90	82	68	51	43	34	25	17	10	6	9	17	29	38	48	62	72	80	87	97	111	123	133
27	236	224	216	207	199	186	173	162	152	143	128	104	97	89	75	57	50	40	31	24	16	10	5	11	22	32	42	56	65	73	80	90	104	116	127
28	243	231	222	213	205	193	180	169	159	150	135	111	103	95	82	64	57	47	38	30	23	16	7	5	16	25	35	49	58	66	74	84	97	109	120
29	249	237	229	220	212	200	187	175	165	157	141	117	110	102	88	71	63	54	44	37	29	22	12	5	9	18	28	42	52	60	67	77	91	103	113
30	256	244	236	227	219	206	193	182	172	163	148	124	117	109	95	77	70	60	51	43	36	29	18	10	4	12	22	36	45	53	60	70	84	96	107
31	263	251	242	233	225	213	200	189	179	170	155	131	123	115	102	84	77	67	58	50	42	35	25	16	5	6	15	29	38	46	54	64	77	89	100
32	269	257	249	240	232	220	207	195	185	177	161	137	130	122	108	91	83	74	64	57	49	42	32	23	11	3	9	22	32	40	47	57	71	83	93
33	276	264	256	247	239	226	213	202	192	183	168	144	137	129	115	97	90	80	71	63	56	48	38	29	18	8	3	16	25	33	40	50	64	76	87
34	283	271	262	253	245	233	220	209	199	190	175	151	143	135	122	104	97	87	78	70	62	55	45	36	24	15	5	9	18	26	34	44	57	70	80
35	289	277	269	260	252	240	227	215	205	197	181	158	150	142	128	111	103	94	84	77	69	62	51	42	31	21	11	3	12	20	27	37	51	63	73
36	296	284	276	267	259	246	233	222	212	204	188	164	157	149	135	117	110	100	91	83	76	68	58	49	38	28	18	4	6	13	21	31	44	56	67
37	303	290	282	273	265	253	240	229	219	210	195	171	163	155	142	124	117	107	98	90	82	75	65	56	44	34	24	10	3	7	14	24	37	50	60
38	309	297	289	280	272	260	247	235	225	217	201	177	170	162	148	131	123	114	104	97	89	82	71	62	51	41	31	17	8	3	8	18	31	43	53
39	316	304	295	286	278	266	253	242	232	223	208	184	176	169	155	137	130	120	111	103	96	88	78	69	57	48	37	23	14	7	5	12	24	36	47
40	322	310	302	293	285	273	260	248	239	230	214	191	183	175	161	144	136	127	117	110	102	95	85	76	64	54	44	30	21	13	7	7	18	30	40
41	329	317	309	300	292	280	266	255	245	237	221	197	190	182	168	150	143	133	124	116	109	101	91	82	71	61	51	37	28	19	13	6	11	23	33
42	336	324	315	306	298	286	273	262	252	243	228	204	196	189	175	157	150	140	131	123	115	108	98	89	77	68	57	43	34	26	19	10	6	17	27
43	342	330	322	313	305	293	280	268	259	250	234	211	203	195	181	164	156	147	137	130	122	115	104	95	84	74	64	50	41	33	26	16	5	11	20
44	349	337	329	320	312	299	286	275	265	257	241	217	210	202	188	170	163	153	144	136	129	121	111	102	91	81	71	57	47	39	32	23	10	6	14
45	356	344	335	326	318	306	293	282	272	263	248	224	216	208	195	177	170	160	151	143	135	128	118	109	97	87	77	63	54	46	39	29	16	6	8
46	362	350	342	333	325	313	300	288	278	270	254	230	223	215	201	184	176	167	157	150	142	135	124	115	104	94	84	70	61	53	45	36	22	11	3
47	369	357	349	340	331	319	306	295	285	276	261	237	230	222	208	190	183	173	164	156	149	141	131	122	110	101	90	76	67	59	52	42	29	17	7

Table EC.6: Arrival rates of logistic vehicles in scenario 1 of the test case

j	1	2	3	4	5	6	7	8	9	10	11	12	13	14	15	16	17	18	19	20
λ_{1j}	0.083	0.078	0.078	0.113	0.118	0.082	0.105	0.07	0.066	0.099	0.117	0.105	0.119	0.116	0.108	0.095	0.092	0.076	0.075	0.088
j	21	22	23	24	25	26	27	28	29	30	31	32	33	34	35					
λ_{1j}	0.098	0.089	0.102	0.076	0.096	0.108	0.107	0.112	0.092	0.097	0.068	0.107	0.103	0.093	0.059					

EC.3 MIP Reformulation of the `MCP Policy`

Let $n \in \{1, \ldots, \bar{n}\}$ denote the maximum number of locations that we aim to reserve. The model selects up to n parking spaces to maximize a concave parking-based utility function. The concavity parameter κ induces diminishing marginal returns for each j, encouraging spatial dispersion of selected parking spaces. The nonlinear objective is reformulated as a mixed-integer linear program via a one-hot encoding of parking space counts.

Decision Variables

$$
\begin{aligned}
x_i &\in \{0,1\} && \forall i \in \mathcal{I} \\
s_j &\in \{0,1,\ldots,n\} && \forall j \in \mathcal{J} \\
y_{jk} &\in \{0,1\} && \forall j \in \mathcal{J},\ k \in \{0,\ldots,n\}
\end{aligned}
$$

`MCP Policy` MIP Model

$$
\max \quad \sum_{j \in \mathcal{J}} \sum_{k=0}^{n} \frac{\lambda_{1j}}{|\delta_j|} k^{\kappa} . y_{jk}. \tag{EC.1a}
$$

$$
s_j = \sum_{i \in \delta_j} x_i \qquad \forall j \in \mathcal{J} \tag{EC.1b}
$$

$$
\sum_{k=0}^{n} y_{jk} = 1 \qquad \forall j \in \mathcal{J} \tag{EC.1c}
$$

$$
s_j = \sum_{k=0}^{n} k . y_{jk} \qquad \forall j \in \mathcal{J} \tag{EC.1d}
$$

$$
\sum_{i \in \mathcal{I}} x_i \leq n \tag{EC.1e}
$$

$$
\mathbf{x}, \mathbf{y} \in \{0,1\},\ \mathbf{s} \in \{0,1,\ldots,n\} \tag{EC.1f}
$$